

1 Title: **Hypoxia regulates endogenous double-stranded RNA production via reduced**
2 **mitochondrial DNA transcription**

3 Esther Arnaiz^{1,2#}, Ana Miar^{1,3#}, Antonio Gregorio Dias Junior^{4,5}, Naveen Prasad³, Ulrike
4 Schulze⁶, Dominic Waithe⁶, Jan Rehwinkel⁴, Adrian L. Harris^{1*}

5 ¹Department of Medical Oncology, Molecular Oncology Laboratories, Weatherall Institute of
6 Molecular Medicine, University of Oxford, John Radcliffe Hospital, Oxford, OX3 9DS, UK

7 ²Current address: Cambridge Institute for Therapeutic Immunology & Infectious Disease,
8 Jeffrey Cheah Biomedical Centre. Puddlecombe Way, Cambridge, CA CB20AW, UK

9 ³Department of Oncology, Old Road Campus Research Building, University of Oxford,
10 Oxford, OX3 7DQ, UK

11 ⁴Medical Research Council Human Immunology Unit, Medical Research Council Weatherall
12 Institute of Molecular Medicine, Radcliffe Department of Medicine, University of Oxford,
13 Oxford OX3 9DS, UK.

14 ⁵Current address: Division of Infectious Diseases and Vaccinology, School of Public Health,
15 University of California, Berkeley, USA.

16 ⁶Radcliffe Department of Medicine, Weatherall Institute of Molecular Medicine, University of
17 Oxford, John Radcliffe Hospital, Oxford, OX3 9DS, UK

18

19 #equal contribution

20 *To whom correspondence should be addressed: Adrian L. Harris Department of Oncology,
21 Weatherall Institute of Molecular Medicine, University of Oxford, John Radcliffe Hospital,
22 OX3 9DS, UK. E-mail: adrian.harris@oncology.ox.ac.uk. Phone: +44 (0)1865 222457 (PA).

23 Short title: Hypoxia effect on dsRNA in cancer

24 This work has been supported by Breast Cancer Now (grant reference 2015MayPR479) and
25 Breast Cancer Research Foundation.

26 Keywords: hypoxia, IFN, dsRNA, mitochondria

27

28 **ABSTRACT:**

29 Hypoxia is a common phenomenon in solid tumours strongly linked to the hallmarks of cancer.
30 Hypoxia promotes local immunosuppression and downregulates type I interferon (IFN)
31 expression and signalling, which contribute to the success of many cancer therapies. Double-
32 stranded RNA (dsRNA), transiently generated during mitochondrial transcription,
33 endogenously activates the type I IFN pathway. We report the effects of hypoxia on the
34 generation of mitochondrial dsRNA (mtdsRNA) in breast cancer. We found a significant
35 decrease in dsRNA production in different cell lines under hypoxia. This was HIF1 α /2 α -
36 independent. mtdsRNA was responsible for induction of type I IFN and significantly decreased
37 after hypoxia. Mitochondrially encoded gene expression was downregulated and mtdsRNA
38 bound by the dsRNA-specific J2 antibody was decreased during hypoxia. These findings
39 reveal a mechanism of hypoxia-induced immunosuppression that could be targeted by
40 hypoxia-activated therapies.

41

42 INTRODUCTION

43 Type I interferons (IFNs) include 13 IFN α subtypes, IFN β , IFN ϵ , IFN κ and IFN ω , and type II
44 and type III IFNs include IFN γ and IFN λ 1-4, respectively. All IFNs are involved in the innate
45 immune response against pathogenic infection. Type I and III IFNs are induced when specific
46 microbial products, known as pathogen-associated molecular patterns (PAMPs), are detected
47 pattern-recognition receptors (PRRs)^{1,2}. PRRs include the Toll-like receptors (TLRs), some of
48 which are specialised to survey the endosomal compartment for nucleic acids. In the cytosol,
49 retinoic acid-inducible gene I (RIG-I) and melanoma differentiation-associated gene 5 (MDA5)
50 detect unusual RNA molecules, while cyclic GMP-AMP (cGAMP) synthase (cGAS) is the
51 major cytosolic double-strand DNA (dsDNA) sensor and activates stimulator of interferon genes
52 (STING).

53 Recognition of viral RNA by RIG-I and MDA5 induces protein conformational changes, which
54 allow interaction with the shared adaptor mitochondrial antiviral-signaling protein (MAVS) that
55 then triggers phosphorylation of interferon-regulatory factor 3 (IRF3) and IRF7. These
56 transcription factors induce the expression of type I and III IFNs, chemokines, inflammatory
57 cytokines and other genes³. All type I IFNs bind a common receptor formed by IFNAR1 and
58 IFNAR2, which through tyrosine kinase 2 (TKY2) and Janus kinase 1 (JAK1) recruits and
59 phosphorylates signal transducer and activator of transcription (STAT) proteins⁴. The canonical
60 IFNAR signalling cascade involves STAT1 and STAT2, which form a ternary complex called
61 interferon-stimulated gene factor 3 (ISGF3) with interferon-regulatory factor 9 (IRF9). ISGF3
62 translocates to the nucleus where it activates the transcription of IFN-stimulated genes (ISGs)².
63 Interestingly, type I IFNs can be produced in the absence of infection and are involved in the
64 success of many anticancer treatments such as radiotherapy, chemotherapy, immunotherapy
65 and oncolytic viruses⁵, promoting direct (tumour cell inhibition) and indirect (antitumour
66 immune response) effects⁶.

67 Hypoxia generates an immunosuppressive microenvironment within the tumour by impeding
68 the homing of immune effector cells and blocking their activity⁷. Additionally, tumours contain
69 more immunosuppressive cells, such as myeloid-derived suppressor cells (MDSCs), tumour-
70 associated macrophages (TAMs) and T-regulatory (Treg) cells, in hypoxic regions^{7,8}.

71 Lactate, generated during the metabolic switch to glycolysis under hypoxia, acts as a ‘signalling
72 molecule’ and attenuates the cytotoxic activity of CTLs⁹ and NK cells¹⁰, helps recruit MDSCs
73 to the tumour¹⁰, and inhibits type I IFN induction via MAVS¹¹.

74 Mitochondrial DNA (mtDNA) is a closed-circular, dsDNA molecule of about 16.6 kb¹². Its
75 complementary DNA strands are called H (heavy) and L (light). The H strand encodes 28
76 genes: 2 rRNAs, 14 tRNAs and 12 polypeptides, whereas the L strand only contains 9 genes
77 encoding for 8 tRNAs and a single polypeptide. Mitochondria generate a number of damage-
78 associated molecular patterns (DAMPs) including ATP, succinate, cardiolipin, N-
79 formylpeptides, mitochondrial transcription factor A (TFAM), cytochrome-c, mtDNA and
80 mitochondrial RNA (mtRNA)¹³. Extracellular mtDNA binds to TRL9¹⁴ whereas cytosolic
81 mtDNA is recognised by inflammasomes¹⁵ and cGAS¹⁶. More recently, mtRNA was described
82 to be a potent DAMP via recognition of a specific segment of the mitochondrial single-strand
83 rRNA by TLR8¹⁷. In addition, dsRNA originating from convergent mtDNA transcription
84 triggers an MDA5-dependent type I IFN response when released to the cytoplasm¹⁸.

85 Previously, we showed that the type I IFN responses induced by exogenous dsRNA are
86 downregulated under hypoxia in cell lines from different solid tumours via transcriptional
87 repression after changes in chromatin conformation¹⁹. Here, we investigated the role of hypoxia
88 in the regulation of endogenous dsRNA formation and function. We have shown that hypoxia
89 decreases the formation of mtdsRNA probably by reducing the mitochondrial transcription
90 rate, and consequently lower endogenous activation of the type I IFN pathway. This effect is

91 HIF1 α /2 α independent and occurs in different cancer cell lines as well as non-transformed cell
92 lines. Moreover, different tissues have different immunostimulatory potential.

93

94 **RESULTS**

95 **Hypoxia prevents the accumulation of immunostimulatory RNAs**

96 Given the immuno-suppressive role of hypoxia, we tested whether cancer cell lines cultured in
97 normoxia or hypoxia contain different amounts of immunostimulatory RNA. We extracted
98 total RNA from the breast cancer cell line MCF7, cultured for 48 hours in normoxia or in 1%
99 or 0.1% hypoxia We then transfected this RNA into an *IFN β* promoter reporter cell line²⁰. RNA
100 from cells grown in normoxia induced expression of the reporter, indicative of the presence of
101 immunostimulatory RNA (fig. 1a). To determine the sensor for this endogenous RNA, we
102 tested the response in reporter cells lacking MDA5, RIG-I or MAVS. This analysis showed
103 that total RNA from MCF7 cells induced an MDA5-MAVS-dependent response (fig 1a).
104 Interestingly, RNA from hypoxic cells (hypoxic RNA) had a significantly reduced capacity to
105 induce activation of the *IFN β* promoter reporter compared with RNA from normoxic cells
106 (normoxic RNA; fig. 1a). Moreover, much like the response to normoxic RNA, residual
107 reporter induction after hypoxic RNA transfection was MDA5-MAVS-dependent and RIG-I-
108 independent (fig. 1a).

109 As 0.1% hypoxia had a greater effect than 1% hypoxia (fig. 1a), subsequent experiments were
110 performed under 0.1% hypoxic conditions. A time course in hypoxia for 4h, 8h, 16h, 24h and
111 48h showed that 4h in hypoxia was enough to lower *IFN β* promoter stimulation and it was
112 maintained up till 48h (fig. 1b left panel). The time course for recovery after reoxygenation
113 following 48h hypoxia was evaluated at 15min, 30min, 1h, 2h, 4h, 8h, 16h and 24h.
114 Reoxygenation caused a gradual recovery of *IFN β* promoter stimulation reaching normoxic
115 basal levels at 24h (fig. 1b right panel).

116 A panel of breast cancer cell lines with different receptor status were used to rule out a cell line
117 dependent effect of hypoxia in MCF7 cells. Hypoxic RNA was much less effective than
118 normoxic RNA in stimulating *IFN β* promoter in all cell lines (fig. 1c).

119

120 **Hypoxic reduction of dsRNA formation is HIF1/2 α independent**

121 Normoxic and hypoxic RNA from 786-0 WT (HIF1 α deficient and HIF2 α upregulated due to
122 *VHL* mutation) and 786-0 HIF2 α KO (hereafter 786-0 KO, HIF1 α and HIF2 α deficient), and
123 RCC4 WT (*VHL* mutation leading to HIF1 α and HIF2 α constitutive overexpression) and RCC4
124 *VHL* (*VHL* restored causing HIF1 α and HIF2 α downregulation) was tested. In both cell lines
125 and all genotypes, hypoxic RNA triggered significantly lower *IFN β* promoter stimulation (fig.
126 1d), highlighting the HIF-independent effect. However, 786-0 KO cells showed higher *IFN β*
127 promoter activation under normoxia compared to 786-0 WT, suggesting an effect of HIF2 α in
128 suppressing *IFN β* induction, although minimal compared to the effect of hypoxia.

129 We also tested normal endothelial cells (HUVECS) and fibroblasts. Again, hypoxic RNA
130 significantly reduced the activation of *IFN β* promoter (fig. 1e) pointing to a general effect of
131 hypoxia independently of cancer.

132 To analyse which RNA species from the total RNA were responsible for the *IFN β* promoter
133 induction, normoxic and hypoxic RNA from MCF7 cells was treated with different RNAses
134 and EMCV (*Encephalomyocarditis Virus*), containing only dsRNA, was used as positive
135 control. RNase III (specific for dsRNA) treatment completely abolished normoxic, hypoxic
136 and EMCV RNA induced *IFN β* promoter activity, whereas RNase A (specific for single-
137 stranded RNA, ssRNA) treatment did not affect the luciferase signal (fig. 1f), showing that
138 endogenous dsRNAs are responsible for the *IFN β* promoter activation rather than ssRNA.

139

140 **Imaging of dsRNA levels downregulation under hypoxia**

141 To visualise the downregulation of dsRNA levels in hypoxia, fluorescence microscopy was
142 performed using the J2 antibody which is widely used to specifically detect dsRNA^{18,21}. There
143 was substantial variability of dsRNA intensity among individual cells, but dsRNA staining was
144 significantly lower in MCF7 hypoxic cells (fig. 2a). The downregulation was time-dependent
145 and significant after 16h in hypoxia (fig. 2b). To confirm the HIF1 α /HIF2 α -independence
146 observed in the *IFN β* promoter assay, 786-0 WT and 786-0 KO cells were stained and both cell
147 lines showed significantly lower dsRNA levels in hypoxia (fig. 2c).

148 **mtDNA and effect of mutation status on dsRNA in hypoxia**

149 It was recently shown that 99% of endogenous dsRNA originates during mtDNA
150 transcription¹⁸. Therefore, we tested cells lacking mtDNA (Rho Zero) and found significantly
151 lower dsRNA staining in the Rho Zero cells than the parental 143B cell line (fig. 3a) and similar
152 reduction in *IFN β* promoter activation (fig. 3b). This strongly suggested that regulation of
153 mitochondria was a key mechanism for hypoxic downregulation of the dsRNA. Surprisingly,
154 there was no difference between normoxia and hypoxia in the 143B parental cell line, either in
155 the dsRNA staining or in the *IFN β* promoter assay. This was the only cell line among all tested
156 in which hypoxia did not downregulate the type I IFN pathway.

157 Differences in metabolism in hypoxic mitochondria were considered a potential contribution
158 to dsRNA release. In hypoxia there is a shift to reductive carboxylation for glutamine utilisation
159 by mitochondria²² and to test this we used U2OS cells harbouring different degrees of
160 heteroplasmy for the mtDNA mutation m8993T>G ranging from 7 to 80% (U2OS mTUNE
161 M7, M45, M80)²³. The basal level of cytoplasmic dsRNA was similar in M7 and M45 (data
162 not shown), as were their metabolic profiles²³, but higher in M80 cells. However, hypoxia
163 downregulated dsRNA levels in all mTUNE cell lines independently of the mutation level (fig.
164 3c) and caused significantly lower *IFN β* promoter activation (fig. 3d).

165 Moreover, it was previously reported that mtdsRNA accumulated and triggered the type I IFN
166 pathway when the degrading enzymes were inhibited (PNPT1, SUV3)¹⁸. However, neither
167 PNPT1 nor SUV3 protein levels were affected by 0.1% hypoxia for 48h (fig. 3e).

168

169 **Hypoxia reduces mtDNA transcription and mitochondrial ribosomal protein (MRP)**
170 **expression**

171 We measured the expression of some mitochondrial encoded genes (*12S*, *ND3*, *ATP6* and
172 *CYTB*) and also nuclear encoded genes involved in mtDNA transcription (*SHMT2*
173 [mitochondrial serine hydroxymethyltransferase involved in the first step of the mitochondrial
174 one-carbon metabolism cleaving serine to glycine], *POLRMT* [mitochondrial RNA polymerase
175 that catalyses mtDNA transcription], *TFAM* [which stabilizes mtDNA, regulates mtDNA
176 transcription, and is required for efficient promoter recognition by *POLRMT*] and *TFB1M*
177 [mitochondrial dimethyladenosine transferase 1 whose interaction with *POLRMT* and *TFAM*
178 is required for mtDNA transcription]). Both sets of genes were significantly downregulated in
179 MCF7 cells cultured under 0.1% hypoxia (fig. 4a). Most of the tested genes showed lower
180 expression after only 4h under hypoxia (*SHMT2*, *POLRMT*, *TFAM*, *ND3*, *ATP6* and *CYTB*)
181 but it was significant for all when cultured for 16h in hypoxia. These results were confirmed
182 by the general downregulation observed in mitochondrial encoded genes and nuclear encoded
183 genes involved in mitochondrial function (from MitoCarta 2.0²⁴) using RNA-seq data from
184 MCF7 cells cultured in normoxia or 0.1% hypoxia for 48h (fig. 4b). As expected, nuclear
185 encoded genes involved in glycolytic metabolism such as pyruvate dehydrogenase kinase 1
186 (*PDK1*) or glyceraldehyde-3-phosphate dehydrogenase (*GAPDH*) were upregulated in
187 hypoxia.

188 We also determined the expression of *POLRMT*, *TFAM* and *TFB1M* and some mitochondrial
189 encoded genes in the parental 143B and Rho zero cells. *12S*, *ND3* and *ATP6* mitochondrial

190 genes were absent in Rho Zero cells whereas *POLRMT*, *TFAM* and *TFB1M* were expressed as
191 previously reported²⁵. However, hypoxia did not show any effect in the parental 143B cell line
192 (Supplementary fig. 1a). This is potentially related to its cytosolic thymidine kinase (TK1)
193 deficiency. Mitochondrial thymidine kinase (TK2) is not cell cycle regulated²⁶. As the cytosolic
194 and mitochondrial thymidine triphosphates are in rapid equilibrium and mainly produced by
195 TK1²⁷, it is possible that there is a more steady state of mtDNA replication, with a stable source
196 of nucleotides from one compartment, which is not cell cycle dependent, in TK1 deficient cells.
197 It was also reported that hypoxia decreased protein expression of mitochondrial ribosomal
198 proteins (MRPs) involved in mtRNA translation²⁸. We tested the expression of the mRNA
199 coding for some of the MRPs under hypoxia in MCF7 cells and found that 16h of hypoxia
200 significantly decreased their expression (fig. 5a). The same trend was observed in 786-0 WT
201 and 786-0 KO cells although it was not always statistically significant (fig. 5b) pointing to a
202 HIF1 α /HIF2 α -independent mechanism.

203 Altogether, these data suggest that hypoxia leads to lower mtDNA transcription and thus lower
204 production of dsRNA available to trigger the type I IFN response.

205

206 **mtRNA is the responsible for the *IFN β* promoter induction**

207 To assess the role of mtdsRNA in inducing the type I IFN pathway, MCF7 cells were cultured
208 in normoxia or 0.1% hypoxia for 48h and their intact mitochondria were isolated. RNA from
209 the mitochondrial and cytosolic fractions was extracted. Firstly, we confirmed that
210 mitochondria were successfully isolated by analysing the expression of several nuclear and
211 mitochondria encoded genes in both fractions (fig. 6a). Nuclear gene expression was detected
212 both in the cytosolic and mitochondrial fractions, suggesting that the mitochondrial fraction
213 could be slightly contaminated with mRNA from the cytoplasm. Nevertheless, the expression
214 of mitochondrial encoded genes was significantly higher in the mitochondrial fraction.

215 Interestingly, mitochondrial encoded genes were downregulated by hypoxia in the
216 mitochondrial fraction but not affected in the cytosolic fraction (fig. 6a).

217 The *IFN β* promoter assay was then performed using these mtRNA and cytosolic RNAs.
218 mtRNA induced *IFN β* promoter stimulation, whereas the luciferase signal using cytosolic RNA
219 was hardly detected. Importantly, hypoxic mtRNA caused significantly lower stimulation of
220 *IFN β* promoter (fig. 6b).

221

222 **dsRNA-enriched fraction in hypoxia showed lower mtRNA content**

223 To assess the composition of the dsRNA pool in hypoxia, dsRNA pull-down was performed
224 using the J2 antibody in MCF7 cells exposed to normoxia or 0.1% hypoxia for 48h, and the
225 resultant RNA was sequenced. Reads were normalised as transcript per million (TPM).
226 Interestingly, the percentage of mitochondrial reads was significantly lower in hypoxia than in
227 normoxia (fig. 6c), and 22 out of 37 mitochondrial encoded genes were significantly
228 downregulated in hypoxia (Supplementary table 1). Density plots in normoxia and hypoxia
229 showed that the non-mitochondrial genes pulled-down by J2 antibody had few reads which
230 probably correspond to background noise (red peak, fig. 6d).

231

232 **Lower mtRNA in hypoxia is not due to increase mitophagy**

233 To evaluate whether the downregulation of mtdsRNA in hypoxia was due mitophagy, we
234 knocked down one of the main genes involved in this process, *BNIP3* (BCL2 Interacting
235 Protein 3) in MCF7 exposed to 0.1% hypoxia for 48h (siBNIP3 and control siRNA, siCON).
236 In the knock-down cells, BNIP3 showed no induction in hypoxia, either at mRNA or protein
237 level. The expression of various ISGs (*DDX58*, *MX1*, *IFIT1*, *IFIT2*, *ADAR-p150* and *ISG15*)
238 was tested. Hypoxia downregulated ISG expression¹⁹, but no differences were found between
239 siCON and siBNIP3 in hypoxia (fig. 7b), suggesting that hypoxic upregulation of BNIP3 does

240 not interfere in the type I IFN signalling. This was further confirmed by the *IFN β* promoter
241 assay, in which hypoxia-induced inhibition on the *IFN β* promoter activation was not recovered
242 upon BNIP3 silencing (fig. 7c).

243 Live cell immunofluorescence was performed using mitochondrial and lysosomal markers in
244 MCF7 cells cultured in normoxia or 0.1% hypoxia for 48h. As previously reported²⁹,
245 mitochondria clearly exhibited morphological changes under low oxygen conditions and
246 appeared more elongated and located closer to the nucleus (fig 7d). However, no colocalization
247 of the mitochondrial and lysosomal markers was observed in normoxia or hypoxia, suggesting
248 that mitophagy is not increased in hypoxia and does not decrease mtdsRNA.

249

250 **Effect of mitochondria-targeting drugs in dsRNA levels**

251 As mitochondria are the main source of dsRNA in the cells¹⁸, the ability of different drugs
252 targeting mitochondria to affect dsRNA levels, as a therapy to overcome hypoxic effects, was
253 assessed in MCF7 cells. Briefly, the drugs used were: chloramphenicol which inhibits
254 mitochondrial protein synthesis via binding to the 50S subunit of the 70S mitochondrial
255 ribosomes; ABT-737 induces cell apoptosis by inhibiting the anti-apoptotic molecule BCL2,
256 as well as mitophagy; G-TPP accumulates in the mitochondria of tumour cells and by inhibiting
257 the heat shock protein 90 (Hsp90) promotes cell apoptosis; mubritinib and metformin decrease
258 mitochondrial respiration by inhibiting ETC complex I; and the Vps34 inhibitor SAR405 alters
259 vesicle trafficking and inhibits autophagy by blocking autophagosome formation.

260 Mubritinib and G-TPP treatment decreased *IFN β* promoter activation under normoxia by 4-
261 and 2-fold, respectively (supplementary fig. 2). Furthermore, hypoxia was not able to further
262 inhibit *IFN β* promoter activity in MCF7 cells treated with these two drugs.

263 Thus, these mitochondrial targeting drugs did not result in increased dsRNA, and although
264 mubritinib and G-TPP inhibited *IFN β* promoter stimulation, hypoxia showed a greater effect.

265 **Tissue distribution of immunostimulatory RNA**

266 Total RNA samples from different human tissues were obtained to assess their effects in the
267 *IFN β* promoter reporter assay. RNA from some tissues including brain, heart, kidney and testis
268 strongly induced the *IFN β* promoter reporter (fig. 8a). In contrast, RNA from other tissues
269 including skeletal muscle and pancreas had little effect. ISG expression was also determined
270 in RNA samples from some tissues. *MX1*, *IFIT1* and *IFNB1* exhibited much higher expression
271 in testis and brain than in skeletal muscle (fig. 8b), confirming the results from the *IFN β*
272 promoter assay.

273

274 **DISCUSSION**

275 In this paper we have shown that hypoxia caused less formation of mtdsRNA in different cancer
276 and normal cell lines leading to lower activation of *IFN β* promoter. This repressive effect was
277 HIF1 α /2 α -independent as hypoxia led to downregulation of mitochondrial gene expression in
278 786-0 HIF2 α -KO cells, as in most other cell lines. However, 786-0 WT cells did not show
279 lower mitochondrial gene expression in hypoxia. Those cells express only HIF2 α , which
280 enhances c-Myc transcriptional activity³⁰ and c-Myc increases the expression of POLRMT,
281 thus increasing mtDNA transcription³¹. Possibly this could compensate for the effect of
282 hypoxia, and other transcription factors such as c-Jun and NF- κ B are noted to have a
283 mitochondrial localisation and can be regulated in hypoxia in a HIF-independent manner³².
284 Endogenous mtRNA and, specifically mtdsRNA, was responsible for triggering the *IFN β*
285 promoter activation via the MDA5/MAVS and not RIG-I/MAVS sensing pathway and the
286 mechanism of reduction in hypoxia was investigated. It was recently reported that 99% of
287 endogenous dsRNA was produced as a consequence of mtDNA transcription, and inhibition of
288 the mtdsRNA degrading enzymes SUV3 and PNPT1 increased type I IFN signalling¹⁸.
289 However, hypoxia did not affect the expression of these degrading enzymes, thus suggesting

290 that lower mtdsRNA presence in hypoxia could be a consequence of lower mitochondrial
291 transcription under low oxygen conditions rather than higher degradation.

292 dsRNA pull-down experiments showed that most of the reads corresponded to the
293 mitochondrial chromosome. However, the percentage of mitochondrial reads was significantly
294 lower in hypoxia and the expression of mitochondrial encoded genes was significantly
295 downregulated. Supporting this hypothesis, we found decreased expression of mitochondrial
296 encoded genes and nuclear encoded genes involved in mitochondrial transcription and
297 mitochondrial ribosomal proteins when cells were cultured for only 4h under hypoxia and it
298 became significant at 16h. Moreover, dsRNA staining was also significantly lower at 16h under
299 hypoxia.

300 Hypoxic-induced mitophagy via BNIP3 was another possible explanation for decreased
301 dsRNA formation^{33,34}. However, our data showed that BNIP3 silencing did not revert the
302 hypoxia-caused downregulation of several ISGs or *IFN β* promoter activation. Moreover, live
303 cell imaging of mitochondria and lysosomes supported this result, as no colocalization of
304 mitochondrial and lysosomal markers was observed either in normoxia or hypoxia.

305 Moreover, we investigated mitochondria-targeting drugs as potential regulators of dsRNA
306 release. Low oxygen concentrations lowered the *IFN β* promoter activation to the same extent
307 as controls for most of the mitochondria-targeting drugs and those inhibitors did not affect
308 normoxic levels. Inhibition of respiration by metformin, a complex I inhibitor, did not affect
309 *IFN β* promoter activation. In contrast, mubritinib and G-TPP, caused a downregulation that
310 reached hypoxic levels, with no further effect of hypoxia. However, mubritinib, which also
311 targets complex I³⁵, is known to inhibit HER2³⁶. HER2 inhibition by trastuzumab increased the
312 expression of pro-apoptotic proteins, which induced the opening of mitochondrial permeability
313 transition pores, ROS production and mitochondrial dysfunction due to loss of mitochondrial
314 membrane potential^{37,38}. Therefore, mubritinib could further contribute to mitochondria

315 dysfunction and the consequent decrease in dsRNA synthesis in MCF7 cells, which have low
316 level of functional HER2^{39,40}. On the other hand, G-TPP specifically inhibits the mitochondrial
317 protein-folding chaperone Hsp90, generating unfolding protein stress in the mitochondria⁴¹
318 which could decrease gene transcription. G-TPP has also been described to induce
319 mitophagy⁴², but as shown above, it is not likely to be the mechanism to decrease dsRNA. The
320 similarity of reduction by these 2 inhibitors to that induced by hypoxia, and lack of further
321 suppression suggest these pathways could overlap e.g. by inhibiting RNA synthesis.

322 Basal levels of dsRNA in different tissues without hypoxic stress was assessed using human
323 total RNA, assuming that the assay measured only dsRNA. RNA from testis, brain, heart and
324 kidney were strong activators of *IFN β* promoter, and these tissues also showed higher
325 expression of type I IFN genes (*MX1*, *IFIT1* and *IFNB1*). Mitochondrial mass is well correlated
326 with citrate synthase and cytochrome oxidase activity, mtDNA copy number and mitochondrial
327 gene expression, and all these parameters are greater in tissues with higher bioenergetics and
328 metabolic demands such as heart⁴³. Although skeletal muscle RNA hardly triggered *IFN β*
329 promoter activation whereas heart RNA was far more effective, this could be explained by low
330 basal activity of mitochondria in resting striated muscle. Additionally, higher oxygen
331 concentrations in tissues such as brain, heart and kidney could stimulate higher turnover⁴⁴.

332 Interestingly, some tumour types such as bladder, breast, esophageal, head and neck, kidney
333 and liver showed significantly lower mtDNA content than paired adjacent normal tissue, and
334 this was associated with lower patient survival⁴⁵. Expression could be even lower in hypoxic
335 areas having impact in anticancer therapies that rely on functional type I IFN signalling.

336 To sum up, we have shown that hypoxia caused significantly lower mtdsRNA production,
337 probably due to a decrease in mitochondrial transcription rather than increased degradation,
338 thus leading to lower activation of *IFN β* promoter, and consequently to lower type I IFN

339 response that could contribute to the immunosuppression observed in hypoxic environments
340 and to chemotherapy and radiotherapy resistance.

341

342 **MATERIALS**

343 Human tissues, cell culture and transfection

344 Human total RNA used in this manuscript was purchased to Takara Bio/Clontech.

345 MCF7, T47D, BT474, MDA-MB-231, MDA-MB-453, MDA-MB-468, RCC4, 786-0, U2OS
346 mTUNE, and human fibroblasts were cultured in DMEM low glucose medium (1g/l; Thermo
347 Fisher Scientific) supplemented with 10% FBS no longer than 20 passages. HUVEC cells were
348 purchased to Lonza and grown in EGM2 medium for maximum 7 passages. They were all
349 mycoplasma tested every 3 months and authenticated during the course of this project. Cells
350 were subjected to 1% or 0.1% hypoxia for the periods specified in each experiment using an
351 InVivO₂ chamber (Baker).

352 U2OS mTUNE glioblastoma cell lines were kindly donated by Dr Christian Frezza. Three
353 isogenic cell lines with different levels of heteroplasmy of mutated mtDNA were used: M7,
354 M45 and M80²³.

355 143B and 143B Rho Zero (Rho Zero) cells were a gift of Dr Karl Morten. Rho Zero cells were
356 generated by treating 143B cells (TK1 deficient) with 10 μ M 2',3'-dideoxycytidine (ddC) for
357 10 days. Both cell lines were grown in high glucose DMEM (Gibco) supplemented with 10%
358 FBS. Rho Zero cell culture media was additionally supplemented with 50 μ g/mL uridine
359 (A15227.06, Alfa Aesar).

360 Drug treatment

361 MCF7 cells were cultured in normoxia or 0.1% hypoxia and treated for 48h with the following
362 mitochondria-targeting drugs: 5 μ M Vps34 inhibitor SAR405 (16979, Cayman Chemical),
363 200 μ M chloramphenicol (C0378, Sigma-Aldrich), 100nM mubritinib (S-2216, Selleckchem),

364 5 μ M ABT-737 (sc-207242, Santa Cruz Biotechnonology), 2mM metformin (D150959, Sigma-
365 Aldrich) or 5 μ M gamitrinib-triphenylphosphonium (G-TPP, HY-102007, MedChemExpress).

366 siRNA transfection

367 BNIP3 siRNA transfection (supplementary table 2) was performed in Optimem reduced serum
368 medium at a final concentration of 5nM, the following day cells were exposed to 0.1% hypoxia
369 for 48h. siRNA control was done in parallel and the following day was subjected to normoxia
370 or 0.1% hypoxia for 48h. Oligofectamine (12252-011, Thermo Fisher Scientific) was used
371 following the manufacturer's instructions.

372 Western blot

373 Whole cell lysates were prepared with RIPA buffer (R0278, Sigma) containing protease
374 (cOmplete, 11697498001) and phosphatase (phosSTOP, 4906845001) inhibitors. Samples
375 were subjected to SDS-PAGE and transferred onto PVDF membranes (IPVH00010,
376 Millipore), after blocking, membranes were incubated overnight with primary antibodies
377 (supplementary table 3) at 4°C. They were later washed and incubated with HRP-anti-
378 mouse/rabbit secondary antibodies (Gibco). Development was performed with Amersham ECL
379 Prime Western Blotting Detection Reagent (GERPN2232, GE Healthcare Life Sciences) using
380 ImageQuantTM LAS 4000. Stripping with Restore PLUS Western Blot Stripping Buffer
381 (46430, Invitrogen) was performed to blot different antibodies in the same membrane.

382 RT-qPCR

383 RNA was extracted using the Tri-Reagent protocol (T9424, Sigma) and 1 μ g was reverse
384 transcribed with the High Capacity cDNA reverse transcription kit (44368813, Thermo Fisher
385 Scientific) using random hexamer primers. The PCR reaction containing SensiMixTM SYBR
386 Green[®] No-ROX Kit (QT650-20, Biorline) was run on a 7900 Real time PCR System (Applied
387 Biosystems) with standard cycling conditions: 10 minutes 95°C, and 40 cycles of 15 seconds

388 95°C followed by 1 minute 60°C. Gene expression was analysed with the Ct method using
389 *HPRT1* expression for normalization. The primers used are listed in Supplementary table 4.

390 *IFN* β promoter reporter assay

391 HEK293T-P125 reporter cells (stably expressing the *IFN* β promoter-Luciferase region²⁰)
392 were used to detect specifically immunostimulatory RNAs as they do not express cGAS and
393 the expression of STING is very low. 4x10⁴ cells per well were seeded in 96-well plates. Next
394 day, cells were pre-treated with 30U/ml of IFN-A/D (I4401, Sigma), and after 24h of
395 incubation fresh medium was added and cells were transfected with 100ng of total RNAs from
396 cell cultures or human tissues using Lipofectamine 2000[®] (11668-019, Thermo Fisher
397 Scientific). As positive controls, 1ng of IVT-RNA or V-EMCV-RNA was used²⁰. 24h post-
398 transfection, cell were lysed and measured using OneGlo luciferase assay (E6120, Promega)
399 in a FluorOPTIMA luminometer.

400 Immunofluorescence for dsRNA

401 Cells were plated on coverslips (VWR Collection) and exposed to 0.1% O₂ hypoxia for 48h.
402 Prior to fixation, mitochondria were stained for 1h with 200nM MitoTracker Deep Red
403 (M22426, Thermo Fisher Scientific). After, cells were washed and fixed with 4% (v/v)
404 paraformaldehyde (PFA) for 8 min at RT. Then, cells were washed and permeabilized with
405 0.1% Triton X-100 for 20 min at RT. PFA was neutralized with 0.1M glycine for 10 min at
406 RT. After washing three times, cells were incubated for 60 min with blocking solution (PBS
407 containing 1% (w/v) BSA and 10% (v/v) normal goat serum (ab7481, Abcam)). Cells were
408 incubated overnight at 4°C in a humidified chamber with J2 primary antibody (10010200,
409 Scicons) at 1:200, and rhodamine phalloidin (R415, Invitrogen) at 1:40 in block solution. Cells
410 were washed three times and incubated with goat anti-mouse IgG Alexa Fluor 488 (R37120,
411 Invitrogen) secondary antibody at 1:500 and Hoechst 33342 (H3570, Invitrogen) at 1:1000
412 concentration in block solution for 1h at RT. After washing three times with PBS, coverslips

413 were mounted with Vectashield® Mounting Medium (H-1000, Vector Labs) and sealed with
414 nail polish.

415 Immunofluorescence dsRNA image analysis

416 Slides were imaged in a Zeiss 880 Inverted confocal microscope (Zeiss) using a 63x Plan-
417 Apochromat objective. Laser properties, acquisition mode and detectors were manually
418 adjusted for each experiment. Fiji Image J software was used for image analysis, using specific
419 macros created by Dr. Ulrike Schulze and Dr. Dominic Waithe. A minimum of 40 cells per
420 condition were analysed.

421 Mitochondria extraction

422 Mitochondria were isolated from MCF7 cells seeded in normoxia or 0.1% hypoxia for 48h
423 using Mitochondria Isolation Kit for Cultured Cells (89874, Thermo Fisher Scientific), and
424 following manufacturer's instructions. Mitochondrial RNA was extracted using Tri Reagent,
425 following the protocol previously explained. 200uL of the cytosolic fraction were also used to
426 extract RNA.

427 Immunoprecipitation of dsRNA

428 Protein G Dynabeads (10004D, Invitrogen) were washed and resuspended in NET-2 buffer.
429 5µg of J2 antibody or mouse IgG2 (400201, BioLegends) were bound to 100µL of beads for
430 1h at RT on a thermoshaker. Conjugated beads were washed three times with NET-2 Buffer.
431 80–90% confluent MCF7 cells from 10cm² plate (×2) were washed with 10 ml of cold PBS.
432 Cells were scraped and transferred to a falcon and spun at 500g at 4°C, 5 min. Cell pellet
433 from one 10cm² plate was lysed in 1 ml of NP-40 lysis buffer and transferred to a tube and
434 incubated on ice for 5 min. Following centrifugation at 17,000g at 4°C for 5 min, supernatant
435 was carefully transferred to a new tube. Total RNA was harvested from 10% input lysate
436 using Tri Reagent. For immunoprecipitation, lysate was supplemented with 10 units of
437 RNase free TurboDNase (AM2238, Ambion) at 10mM MgCl₂ per 1 mL of mix. 100µL of

438 J2-Dynabeads was added to 1mL of above lysate and left for 1–2h at 4°C. Following
439 magnetic separation, beads were washed twice with 1mL of high salt washing buffer
440 (HSWB). Beads were transferred to a new tube with NET-2 buffer and washed twice with
441 the same buffer. J2-bound dsRNA was extracted with Tri Reagent. The RNA samples were
442 sent for sequencing. NET-2 buffer (50mM Tris-Cl, pH 7.4, 150mM NaCl, 1mM MgCl₂,
443 0.5% NP-40), NP-40 lysis buffer (50mM Tris-Cl pH 7.4, 150mM NaCl, 5mM EDTA, 0.5%
444 NP-40), high salt wash buffer (50mM Tris-Cl pH 7.4, 1M NaCl, 1mM EDTA, 1% NP-40,
445 0.5% DOC, 0.1% SDS).

446 RNA-sequencing and data analysis

447 Libraries for paired end sequencing were prepared using standard Illumina protocol and
448 sequencing was performed using Illumina NovoSeq 6000 sequencer at Wellcome Centre for
449 Human Genetics. Raw reads were processed using FASTQC and Cutadapt and aligned to the
450 genome using STAR. Normalised counts of nuclear encoded genes involved in mitochondrial
451 function and mitochondrial encoded genes were used for generation of heatmaps. In order to
452 estimate the proportion of counts that map to mitochondrial and non-mitochondrial genes;
453 transcript per million (TPM) normalized value of transcripts encoded by mitochondrial and non
454 mitochondrial genome in different replicates was calculated. Proportion of TPM counts in
455 mitochondrial or non-mitochondrial fractions was calculated by dividing the sum of TPM
456 counts in the fraction by total TPM counts.

457 Statistical analysis

458 GraphPad Prism 8.0 statistical analysis software (GraphPad Software) was used. If not
459 otherwise specified, all the experiments were performed in 3 biological triplicates. ANOVA or
460 ANOVA on ranks was normally used to study one variable in more than 2 groups depending
461 on if they follow a normal distribution or not respectively. When two means were compared,
462 t-test was performed if samples followed a normal distribution or Mann-Whitney if there was

463 not a normal distribution. When analysing the influence of two different independent variables
464 on one dependent variable, 2-way ANOVA was applied. In the graphs, the error bars depict the
465 standard error of the mean (SEM).

466

467 **DATA AVAILABILITY**

468 RNA-seq data is available in the Gene Expression Omnibus (GSE153557).

469

470

471

472

473

474

475

476

477

478

479

480

481

482

483

484

485

486

487

488

489 References

- 490 1 Rehwinkel, J. & Gack, M. U. RIG-I-like receptors: their regulation and roles in RNA sensing. *Nat*
491 *Rev Immunol*, doi:10.1038/s41577-020-0288-3 (2020).
- 492 2 McNab, F., Mayer-Barber, K., Sher, A., Wack, A. & O'Garra, A. Type I interferons in infectious
493 disease. *Nat Rev Immunol* **15**, 87-103, doi:10.1038/nri3787 (2015).
- 494 3 Honda, K., Takaoka, A. & Taniguchi, T. Type I interferon [corrected] gene induction by the
495 interferon regulatory factor family of transcription factors. *Immunity* **25**, 349-360,
496 doi:10.1016/j.immuni.2006.08.009 (2006).
- 497 4 Stark, G. R. & Darnell, J. E., Jr. The JAK-STAT pathway at twenty. *Immunity* **36**, 503-514,
498 doi:10.1016/j.immuni.2012.03.013 (2012).
- 499 5 Zitvogel, L., Galluzzi, L., Kepp, O., Smyth, M. J. & Kroemer, G. Type I interferons in anticancer
500 immunity. *Nat Rev Immunol* **15**, 405-414, doi:10.1038/nri3845 (2015).
- 501 6 Budhwani, M., Mazzieri, R. & Dolcetti, R. Plasticity of Type I Interferon-Mediated Responses
502 in Cancer Therapy: From Anti-tumor Immunity to Resistance. *Front Oncol* **8**, 322,
503 doi:10.3389/fonc.2018.00322 (2018).
- 504 7 Noman, M. Z. *et al.* Hypoxia: a key player in antitumor immune response. A Review in the
505 Theme: Cellular Responses to Hypoxia. *Am J Physiol Cell Physiol* **309**, C569-579,
506 doi:10.1152/ajpcell.00207.2015 (2015).
- 507 8 Noman, M. Z. *et al.* Microenvironmental hypoxia orchestrating the cell stroma cross talk,
508 tumor progression and antitumor response. *Crit Rev Immunol* **31**, 357-377 (2011).
- 509 9 Feder-Mengus, C. *et al.* Multiple mechanisms underlie defective recognition of melanoma
510 cells cultured in three-dimensional architectures by antigen-specific cytotoxic T lymphocytes.
511 *Br J Cancer* **96**, 1072-1082, doi:10.1038/sj.bjc.6603664 (2007).
- 512 10 Husain, Z., Huang, Y., Seth, P. & Sukhatme, V. P. Tumor-derived lactate modifies antitumor
513 immune response: effect on myeloid-derived suppressor cells and NK cells. *J Immunol* **191**,
514 1486-1495, doi:10.4049/jimmunol.1202702 (2013).
- 515 11 Zhang, W. *et al.* Lactate Is a Natural Suppressor of RLR Signaling by Targeting MAVS. *Cell* **178**,
516 176-189 e115, doi:10.1016/j.cell.2019.05.003 (2019).
- 517 12 Andrews, R. M. *et al.* Reanalysis and revision of the Cambridge reference sequence for human
518 mitochondrial DNA. *Nat Genet* **23**, 147, doi:10.1038/13779 (1999).
- 519 13 Pallen, M. J. Time to recognise that mitochondria are bacteria? *Trends Microbiol* **19**, 58-64,
520 doi:10.1016/j.tim.2010.11.001 (2011).
- 521 14 Zhang, Q. *et al.* Circulating mitochondrial DAMPs cause inflammatory responses to injury.
522 *Nature* **464**, 104-107, doi:10.1038/nature08780 (2010).
- 523 15 Zhou, R., Yazdi, A. S., Menu, P. & Tschopp, J. A role for mitochondria in NLRP3 inflammasome
524 activation. *Nature* **475**, 122, doi:10.1038/nature10156 (2011).
- 525 16 Rongvaux, A. *et al.* Apoptotic caspases prevent the induction of type I interferons by
526 mitochondrial DNA. *Cell* **159**, 1563-1577, doi:10.1016/j.cell.2014.11.037 (2014).
- 527 17 Krüger, A. *et al.* Human TLR8 senses UR/URR motifs in bacterial and mitochondrial RNA. *EMBO*
528 *reports* **16**, 1656-1663, doi:10.15252/embr.201540861 (2015).
- 529 18 Dhir, A. *et al.* Mitochondrial double-stranded RNA triggers antiviral signalling in humans.
530 *Nature* **560**, 238-242, doi:10.1038/s41586-018-0363-0 (2018).
- 531 19 Miar, A. *et al.* Hypoxia induces transcriptional and translational downregulation of the type I
532 interferon (IFN) pathway in multiple cancer cell types. *bioRxiv*, 715151, doi:10.1101/715151
533 (2019).
- 534 20 Hertzog, J. *et al.* Infection with a Brazilian isolate of Zika virus generates RIG-I stimulatory RNA
535 and the viral NS5 protein blocks type I IFN induction and signaling. *Eur J Immunol* **48**, 1120-
536 1136, doi:10.1002/eji.201847483 (2018).
- 537 21 Burger, K. *et al.* Nuclear phosphorylated Dicer processes double-stranded RNA in response to
538 DNA damage. *J Cell Biol* **216**, 2373-2389, doi:10.1083/jcb.201612131 (2017).

- 539 22 Eales, K. L., Hollinshead, K. E. & Tennant, D. A. Hypoxia and metabolic adaptation of cancer
540 cells. *Oncogenesis* **5**, e190, doi:10.1038/oncsis.2015.50 (2016).
- 541 23 Gaude, E. *et al.* NADH Shuttling Couples Cytosolic Reductive Carboxylation of Glutamine with
542 Glycolysis in Cells with Mitochondrial Dysfunction. *Mol Cell* **69**, 581-593.e587,
543 doi:10.1016/j.molcel.2018.01.034 (2018).
- 544 24 Calvo, S. E., Clauser, K. R. & Mootha, V. K. MitoCarta2.0: an updated inventory of mammalian
545 mitochondrial proteins. *Nucleic Acids Res* **44**, D1251-1257, doi:10.1093/nar/gkv1003 (2016).
- 546 25 Wilson, W. L. & LeBelle, M. J. Identification of an imidazolinium salt, the major product from
547 reaction of benzathine with iodine. *J Pharm Sci* **68**, 1322-1323, doi:10.1002/jps.2600681035
548 (1979).
- 549 26 King, M. P. & Attardi, G. Human cells lacking mtDNA: repopulation with exogenous
550 mitochondria by complementation. *Science* **246**, 500-503, doi:10.1126/science.2814477
551 (1989).
- 552 27 Pontarin, G., Gallinaro, L., Ferraro, P., Reichard, P. & Bianchi, V. Origins of mitochondrial
553 thymidine triphosphate: dynamic relations to cytosolic pools. *Proc Natl Acad Sci U S A* **100**,
554 12159-12164, doi:10.1073/pnas.1635259100 (2003).
- 555 28 Bousquet, P. A. *et al.* Hypoxia Strongly Affects Mitochondrial Ribosomal Proteins and
556 Translocases, as Shown by Quantitative Proteomics of HeLa Cells. *Int J Proteomics* **2015**,
557 678527, doi:10.1155/2015/678527 (2015).
- 558 29 Chiche, J. *et al.* Hypoxic enlarged mitochondria protect cancer cells from apoptotic stimuli.
559 *Journal of cellular physiology* **222**, 648-657, doi:10.1002/jcp.21984 (2010).
- 560 30 Gordan, J. D., Bertout, J. A., Hu, C. J., Diehl, J. A. & Simon, M. C. HIF-2alpha promotes hypoxic
561 cell proliferation by enhancing c-myc transcriptional activity. *Cancer Cell* **11**, 335-347,
562 doi:10.1016/j.ccr.2007.02.006 (2007).
- 563 31 Oran, A. R. *et al.* Multi-focal control of mitochondrial gene expression by oncogenic MYC
564 provides potential therapeutic targets in cancer. *Oncotarget* **7**, 72395-72414,
565 doi:10.18632/oncotarget.11718 (2016).
- 566 32 Barshad, G., Marom, S., Cohen, T. & Mishmar, D. Mitochondrial DNA Transcription and Its
567 Regulation: An Evolutionary Perspective. *Trends Genet* **34**, 682-692,
568 doi:10.1016/j.tig.2018.05.009 (2018).
- 569 33 Sowter, H. M., Ratcliffe, P. J., Watson, P., Greenberg, A. H. & Harris, A. L. HIF-1-dependent
570 regulation of hypoxic induction of the cell death factors BNIP3 and NIX in human tumors.
571 *Cancer Res* **61**, 6669-6673 (2001).
- 572 34 Zhang, H. *et al.* Mitochondrial autophagy is an HIF-1-dependent adaptive metabolic response
573 to hypoxia. *J Biol Chem* **283**, 10892-10903, doi:10.1074/jbc.M800102200 (2008).
- 574 35 Baccelli, I. *et al.* Mubritinib Targets the Electron Transport Chain Complex I and Reveals the
575 Landscape of OXPHOS Dependency in Acute Myeloid Leukemia. *Cancer cell* **36**, 84-99.e88,
576 doi:10.1016/j.ccell.2019.06.003 (2019).
- 577 36 Nagasawa, J. *et al.* Novel HER2 selective tyrosine kinase inhibitor, TAK-165, inhibits bladder,
578 kidney and androgen-independent prostate cancer in vitro and in vivo. *International journal*
579 *of urology : official journal of the Japanese Urological Association* **13**, 587-592,
580 doi:10.1111/j.1442-2042.2006.01342.x (2006).
- 581 37 Gorini, S. *et al.* Chemotherapeutic Drugs and Mitochondrial Dysfunction: Focus on
582 Doxorubicin, Trastuzumab, and Sunitinib. *Oxidative medicine and cellular longevity* **2018**,
583 7582730, doi:10.1155/2018/7582730 (2018).
- 584 38 Stagg, J. *et al.* Anti-ErbB-2 mAb therapy requires type I and II interferons and synergizes with
585 anti-PD-1 or anti-CD137 mAb therapy. *Proceedings of the National Academy of Sciences* **108**,
586 7142-7147, doi:10.1073/pnas.1016569108 (2011).
- 587 39 Wu, C. H. *et al.* Estradiol induces cell proliferation in MCF7 mammospheres through
588 HER2/COX2. *Mol Med Rep* **19**, 2341-2349, doi:10.3892/mmr.2019.9879 (2019).

- 589 40 Li, X. *et al.* Posttranscriptional upregulation of HER3 by HER2 mRNA induces trastuzumab
590 resistance in breast cancer. *Mol Cancer* **17**, 113, doi:10.1186/s12943-018-0862-5 (2018).
- 591 41 Kang, B. H. *et al.* Combinatorial drug design targeting multiple cancer signaling networks
592 controlled by mitochondrial Hsp90. *The Journal of clinical investigation* **119**, 454-464,
593 doi:10.1172/jci37613 (2009).
- 594 42 Fiesel, F. C., James, E. D., Hudec, R. & Springer, W. Mitochondrial targeted HSP90 inhibitor
595 Gamitrinib-TPP (G-TPP) induces PINK1/Parkin-dependent mitophagy. *Oncotarget* **8**, 106233-
596 106248, doi:10.18632/oncotarget.22287 (2017).
- 597 43 D'Erchia, A. M. *et al.* Tissue-specific mtDNA abundance from exome data and its correlation
598 with mitochondrial transcription, mass and respiratory activity. *Mitochondrion* **20**, 13-21,
599 doi:10.1016/j.mito.2014.10.005 (2015).
- 600 44 Krysko, D. V. *et al.* Emerging role of damage-associated molecular patterns derived from
601 mitochondria in inflammation. *Trends Immunol* **32**, 157-164, doi:10.1016/j.it.2011.01.005
602 (2011).
- 603 45 Reznik, E. *et al.* Mitochondrial DNA copy number variation across human cancers. *Elife* **5**,
604 doi:10.7554/eLife.10769 (2016).

605

606 **ACKNOWLEDGEMENTS**

607 We thank Dr Karl Morten (University of Oxford, UK) for the 143B and Rho Zero cells, Dr
608 Charles Lawrie (Biodonostia Instituto de Investigación Sanitaria, Spain) for the 786-0 WT and
609 HIF2 α -KO cells, and Dr Christian Frezza (University of Cambridge, UK) for the mTUNE cells.

610

611 **AUTHOR CONTRIBUTION**

612 EA, AM, JR and ALH designed the experiments, analysed the data and wrote the manuscript.
613 AM and EA performed the experiments. AGDJ developed the *IFN β* promoter assay and
614 performed this assay for fig. 1a and fig. 8a. US and DW developed the ImageJ macro to
615 quantify J2 immunofluorescence. NP performed all RNA-seq and J2-IP analysis. This research
616 was supported by funding from Cancer Research UK (ALH), Breast Cancer Research
617 Foundation (ALH), and Breast Cancer Now (ALH, AM).

618 **Competing interests statement:** Authors have nothing to declare.

619

620

621 **FIGURE LEGENDS**

622 **Figure 1. Hypoxia decreased *IFN β* promoter stimulation.** a) An outline of the experiment
623 is shown (top, please see text for detail). *IFN β* promoter reporter cells of the indicated
624 genotypes were transfected with total RNA extracted from MCF7 cells exposed for 48h to
625 normoxia, 1% hypoxia and 0.1% hypoxia. 24h after transfection, reporter cells were lysed
626 and firefly luciferase activity was determined (bar charts; RLU, relative light units). Data
627 from control cells treated with transfection reagent only were used to calculate RLU fold
628 changes after RNA transfection (n=10). b) *IFN β* promoter stimulation time course using
629 RNA from MCF7 cells exposed to normoxia or 0.1% hypoxia for 4h, 8h, 16h, 24h and 48h
630 (left panel, n=3), and reoxygenation for 15min, 30min, 1h, 2h, 4h, 8h, 16h and 24h after 48h
631 in 0.1% hypoxia (right panel, n=3). c) *IFN β* promoter stimulation using RNA from a panel of
632 breast cancer cell lines exposed to normoxia or 0.1% hypoxia for 48h. d) *IFN β* promoter
633 stimulation using RNA from 786-0 WT or 786-0 HIF2 α KO cells (786-0 KO, left panel,
634 n=3), and RCC4 EV or RCC4 VHL (right panel, n=3) exposed to normoxia or 0.1% hypoxia
635 for 48h. e) *IFN β* promoter stimulation using RNA from non cancerous cell lines exposed to
636 normoxia or 0.1% hypoxia for 48h (n=3). f) *IFN β* promoter stimulation using RNA from
637 MCF7 cells treated with RNase A or RNase III, and EMCV dsRNA as positive control
638 (n=3). Number of replicates indicate biological replicates and data is shown as mean \pm SEM. *
639 p<0.05, ** p<0.01, *** p<0.001.

640 **Figure 2. dsRNA staining is significantly lower under hypoxia independently of**
641 **HIF1 α /2 α expression.** a) dsRNA was stained using J2 antibody in MCF7 cells exposed to
642 normoxia (n=45 cells) or 0.1% hypoxia (n=45 cells) for 48h from 3 independent replicates. b)
643 dsRNA was monitored during a time course of MCF7 cells in normoxia (n=40 cells), or
644 exposed to 0.1% for 4h (n=40 cells), 16h (n=40 cells), and 48h (n=40 cells) from 3

645 independent replicates. c) HIF1 α /2 α involvement was evaluated by staining dsRNA in 786-0
646 WT cells (786 WT, n=46 normoxic cells and n=46 hypoxic cells), and 786-0 HIF2 α -KO cells
647 (786 KO, n= 45 normoxic cells and n=45 hypoxic cells) from 3 independent replicates. Data
648 is shown as mean \pm SEM. * p<0.05, ** p<0.01, *** p<0.001. Green: J2 antibody staining,
649 blue: DAPI, and red: mitotracker staining. Scale bars correspond to 10 μ m.

650 **Figure 3. Mitochondrial alterations did not affect dsRNA staining reduction under**
651 **hypoxia.** a) Representative images showing dsRNA staining using J2 antibody in 143B WT
652 cells in normoxia (n=44 cells) or 0.1% hypoxia (n=42 cells) for 48h and in 143B lacking
653 mtDNA (Rho Zero) exposed to normoxia (n=40 cells) from 3 independent replicates. b) *IFN β*
654 promoter stimulation was evaluated as explained in fig.1a using RNA from 143B WT and
655 Rho Zero cells cultured in normoxia and 0.1% hypoxia for 48h (n=3; RLU, relative light
656 units). c) Representative images showing dsRNA staining in U2OS isogenic lines harbouring
657 7% vs 80% of heteroplasmy for the mtDNA mutation m8993T>G (mTUNE M7 normoxia
658 n=40 cells and 0.1% hypoxia n=40 cells, M80 normoxia n=40 cells and 0.1% hypoxia n=40
659 cells) from 3 independent replicates. d) *IFN β* promoter stimulation using RNA from mTUNE
660 M7, M45 and M80 cells in normoxia and 0.1% hypoxia for 48h (n=3). e) Western blot
661 showing PNPT1 and SUV3 dsRNA degrading enzymes protein levels in normoxia and
662 hypoxia (n=3). Number of replicates indicate biological replicates and data is shown as
663 mean \pm SEM. * p<0.05, ** p<0.01, *** p<0.001. Green: J2 antibody staining, blue: DAPI, and
664 red: mitotracker staining. Scale bars correspond to 10 μ m.

665 **Figure 4. Hypoxia downregulates the expression of mitochondrial genes.** a) RNA
666 expression of mitochondrial encoded genes (*12S*, *ND3*, *ATP6*, *CYT6*) or nuclear encoded
667 genes involved in mitochondrial function (*SHMT2*, *POLRMT*, *TFAM*, *TFB1M*) in MCF7 cells
668 cultured in normoxia or 0.1% hypoxia for 4h, 8h, 16h, 24h and 48h was evaluated by qPCR
669 (n=3). b) Heatmap showing expression of mitochondrial encoded genes (right panel) or 1158

670 nuclear encoded genes involved in mitochondrial function (left panel, from MitoCarta 2.0) in
671 MCF7 cells cultured in normoxia or 0.1% hypoxia for 48h (n=3) from RNAseq experiment
672 described in Materials section. Number of replicates indicate biological replicates and data is
673 shown as mean±SEM. * p<0.05, ** p<0.01, *** p<0.001

674 **Figure 5. Expression of mitochondrial ribosomal proteins (MRPs) is downregulated**
675 **under hypoxia.** a) RNA expression of MRPs involved in mtRNA translation in MCF7 cells
676 cultured in normoxia or 0.1% hypoxia for 4h, 8h, 16h, 24h and 48h was evaluated by qPCR
677 (n=3). b) MRPs mRNA expression in 786-0 WT and 786-0 KO cells cultured in normoxia or
678 0.1% hypoxia for 48h was also evaluated by qPCR (n=3). Number of replicates indicate
679 biological replicates and data is shown as mean±SEM. * p<0.05, ** p<0.01, *** p<0.001

680 **Figure 6. Mitochondrial RNA is responsible for *IFNβ* promoter activation.** a) MCF7
681 cells cultured in normoxia and 0.1% hypoxia for 48h were fractionated. RNA expression of
682 mitochondrial (*12S*, *CYTB*, *ATP6*) and nuclear encoded genes (*POLRMT*, *TFAM*, *TFB1M*) in
683 mitochondrial and cytosolic fractions is shown by qPCR (n=3). Note difference in axes for
684 mitochondrial versus nuclear genes. b) RNA from a) was used to activate the *IFNβ* promoter
685 as described in fig. 1a (n=3; RLU, relative light units). c) dsRNA pull down experiment
686 using J2 antibody in MCF7 cells exposed to normoxia or 0.1% hypoxia for 48h was
687 performed. Bar graph shows proportion of transcripts per million (TPM) mitochondrial and
688 non-mitochondrial reads (n=3). d) Density plots show mitochondrial (green), non-
689 mitochondrial (red) and all reads (blue) in each replicate (rep) obtained from the dsRNA pull-
690 down experiment in b) (n=3). Number of replicates indicate biological replicates and data is
691 shown as mean±SEM. * p<0.05, ** p<0.01, *** p<0.001

692 **Figure 7. Mitophagy is not involved in mtdsRNA reduction under hypoxia.** a) Silencing
693 of BNIP3 was confirmed by qPCR (left panel) and western blot (right panel) in siBNIP3

694 MCF7 cells in hypoxia vs control (siCON) (n=3). b) RNA expression of IFN-induced genes
695 (ISGs) in siBNIP3 MCF7 cells vs siCON was performed by qPCR (n=3). c) RNA from a)
696 was used to evaluate *IFN β* promoter activation after BNIP3 silencing (n=3; RLU, relative
697 light units). d) Representative image showing lack of colocalization between the
698 mitochondrial (green) and lysosomal (red) markers in MCF7 cells exposed to normoxia or
699 0.1% hypoxia for 48h (n=3). Number of replicates indicate biological replicates and data is
700 shown as mean \pm SEM. * p<0.05, ** p<0.01, *** p<0.001

701 **Figure 8. Level of type I IFN pathway activation is tissue-dependent.** a) The *IFN β*
702 promoter reporter assay shown in Fig. 1a was used to assess the immunostimulatory
703 properties of RNA samples from different tissues (n=3). b) qPCR showing expression of
704 *MX1*, *IFIT1* and *IFN β* in different tissues from a) (n=3). Number of replicates indicate
705 biological replicates and data is shown as mean \pm SEM.

706

Figure 1

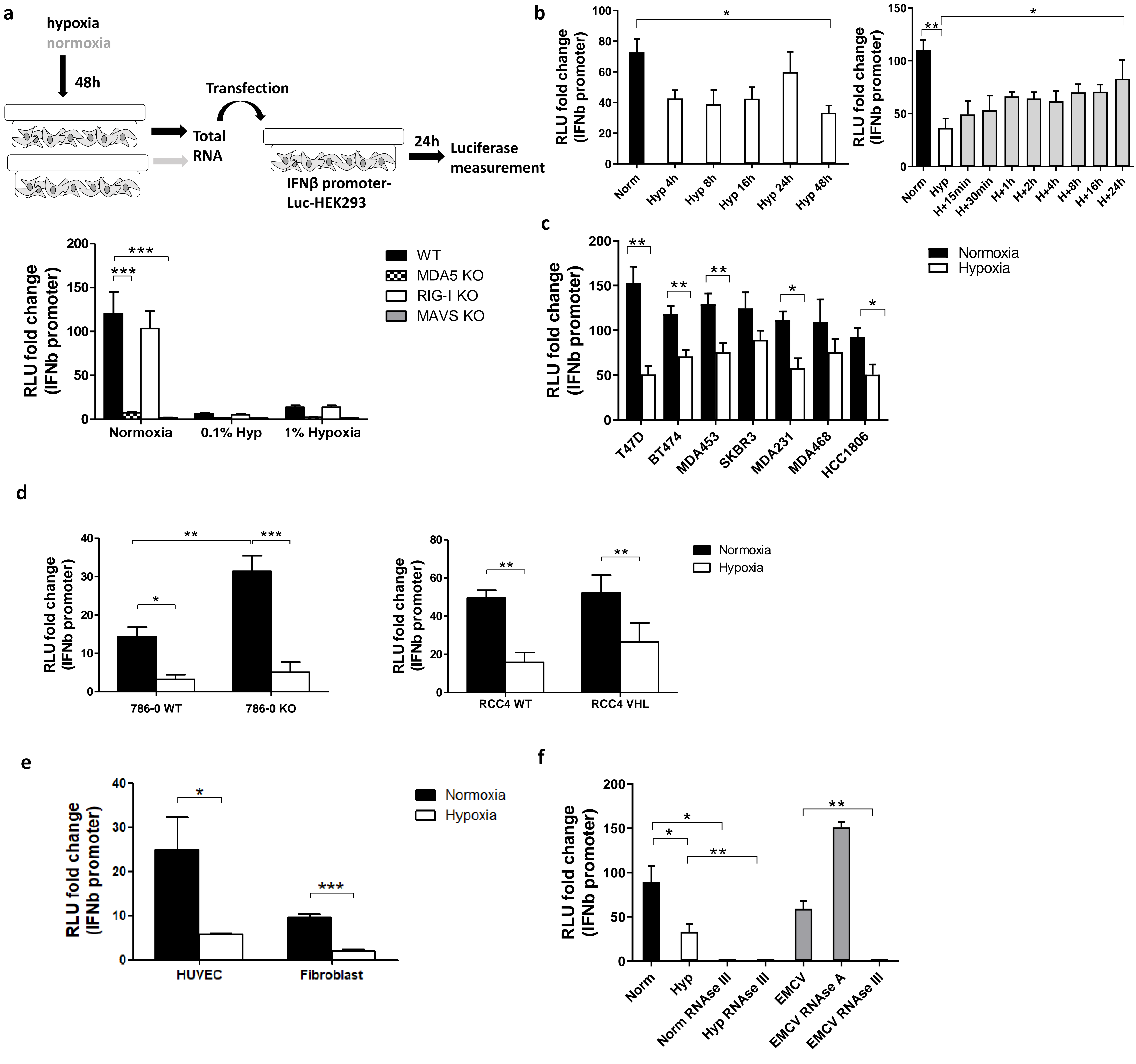
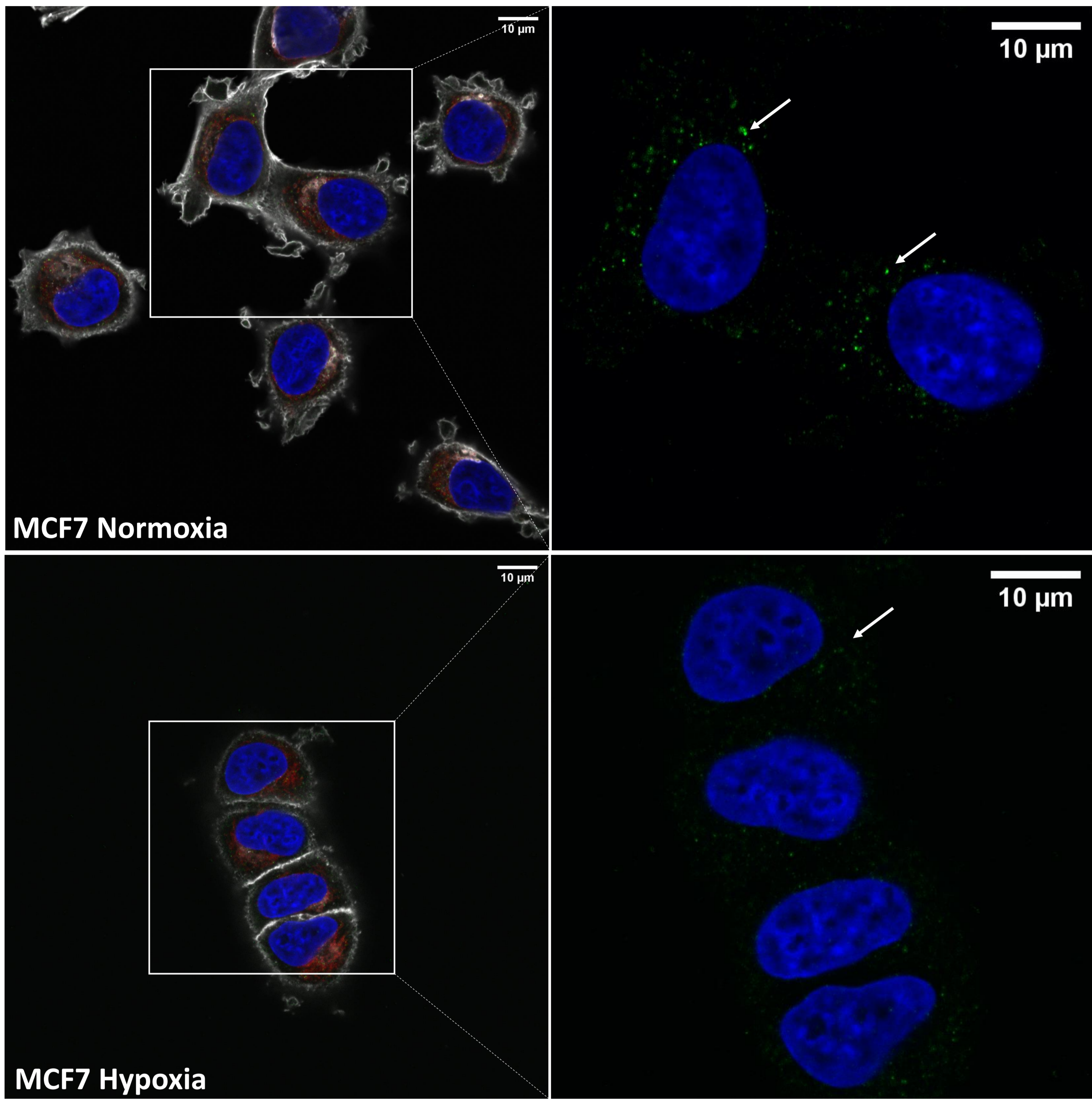
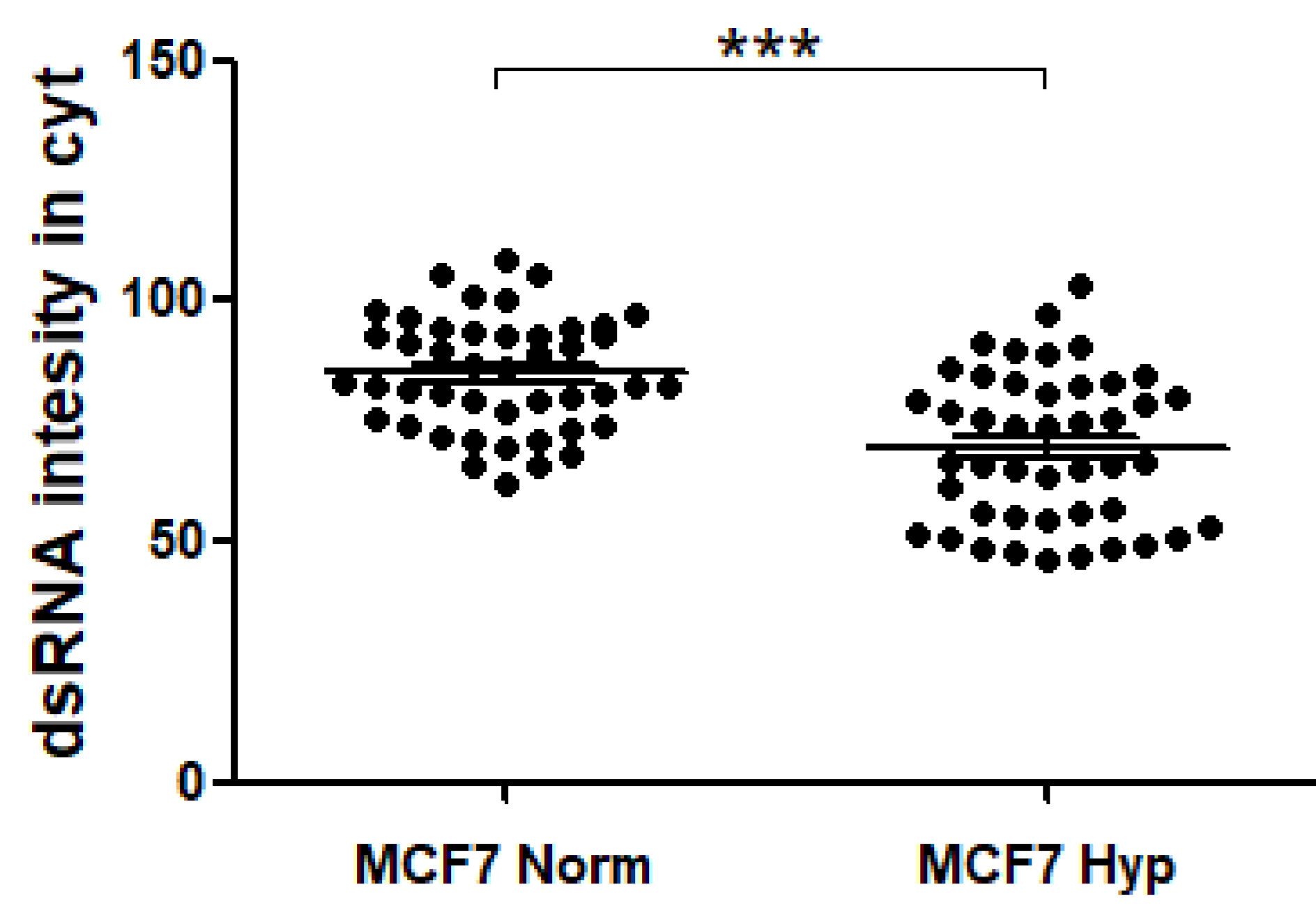
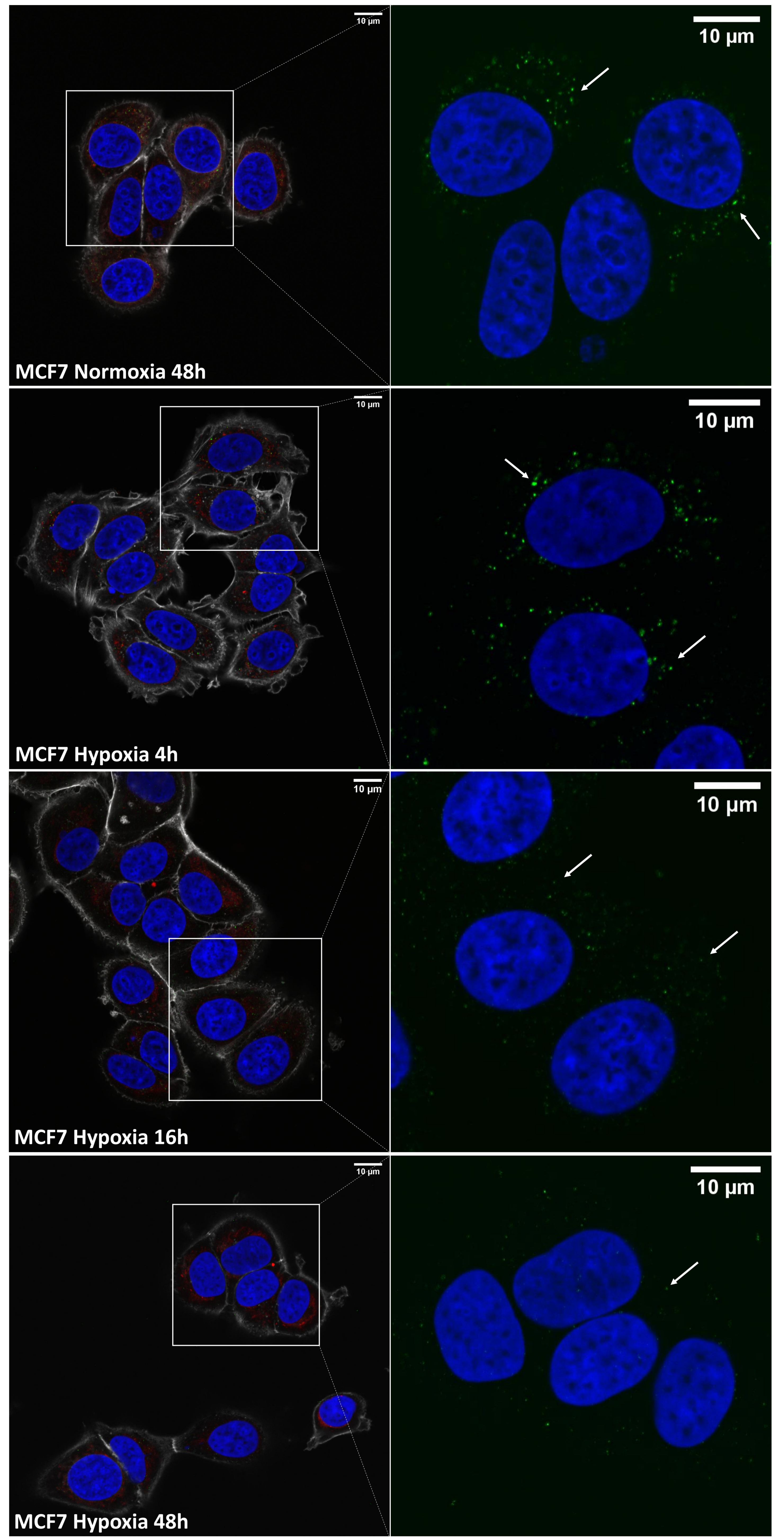
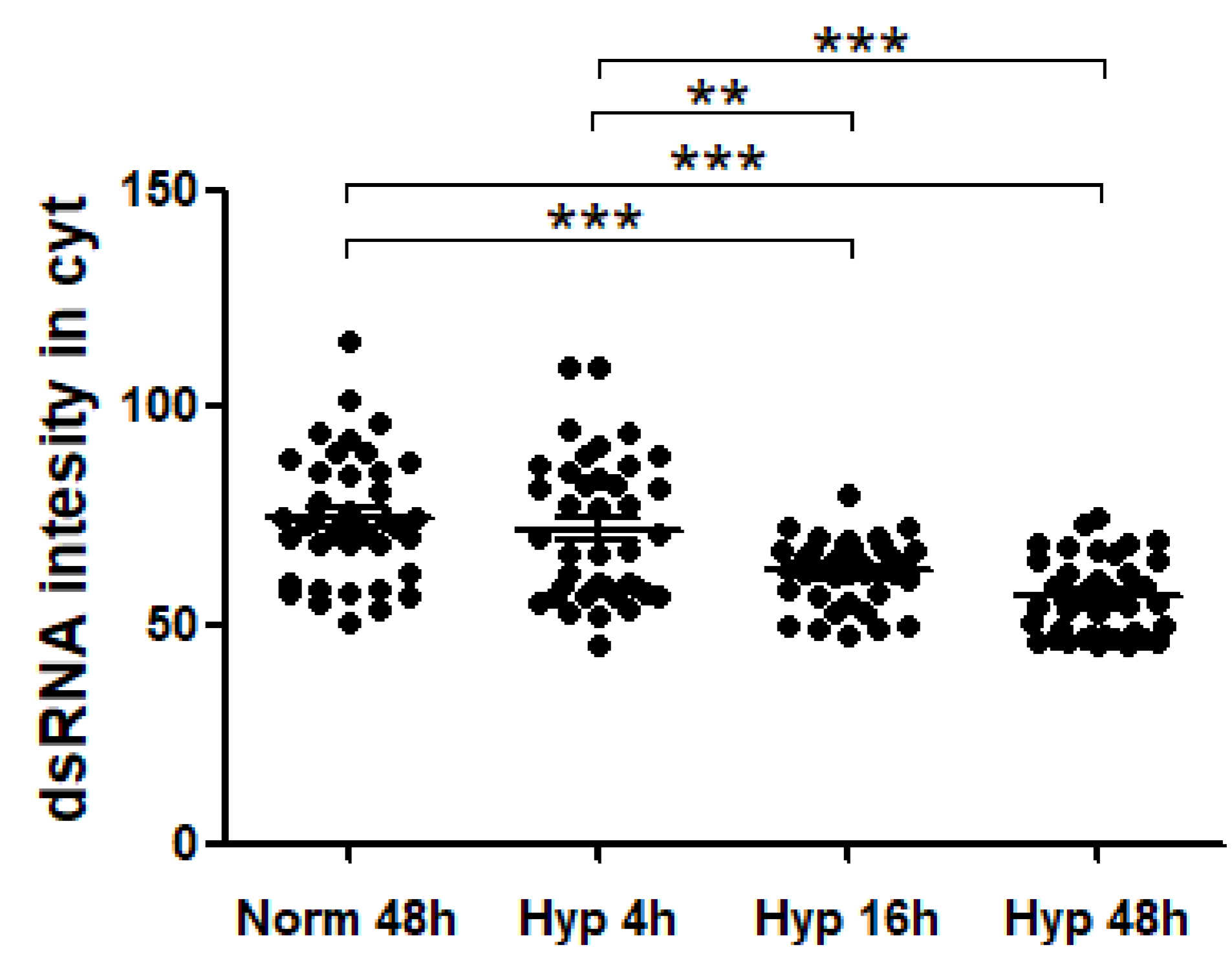


Figure 2

a



b



c

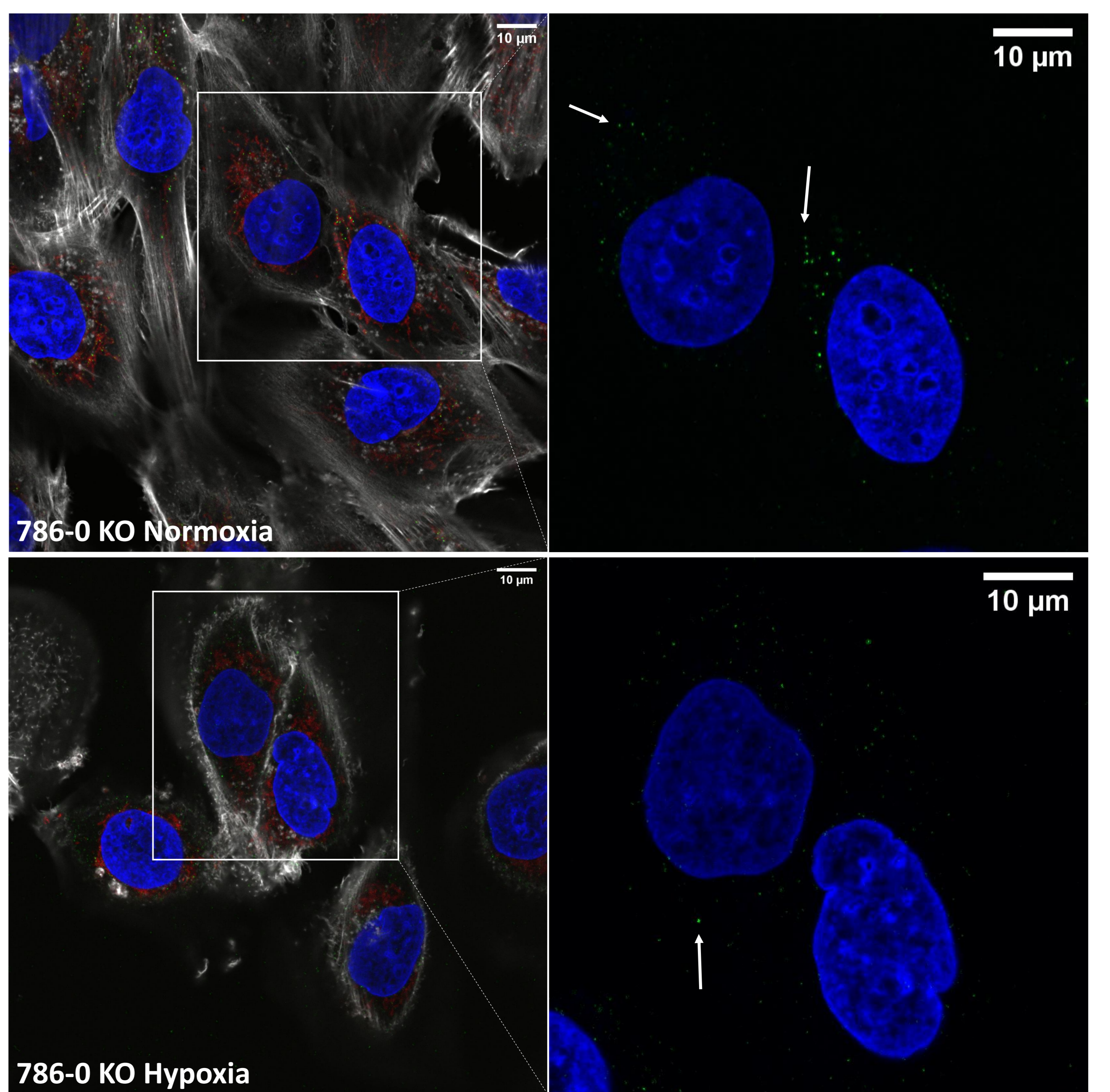
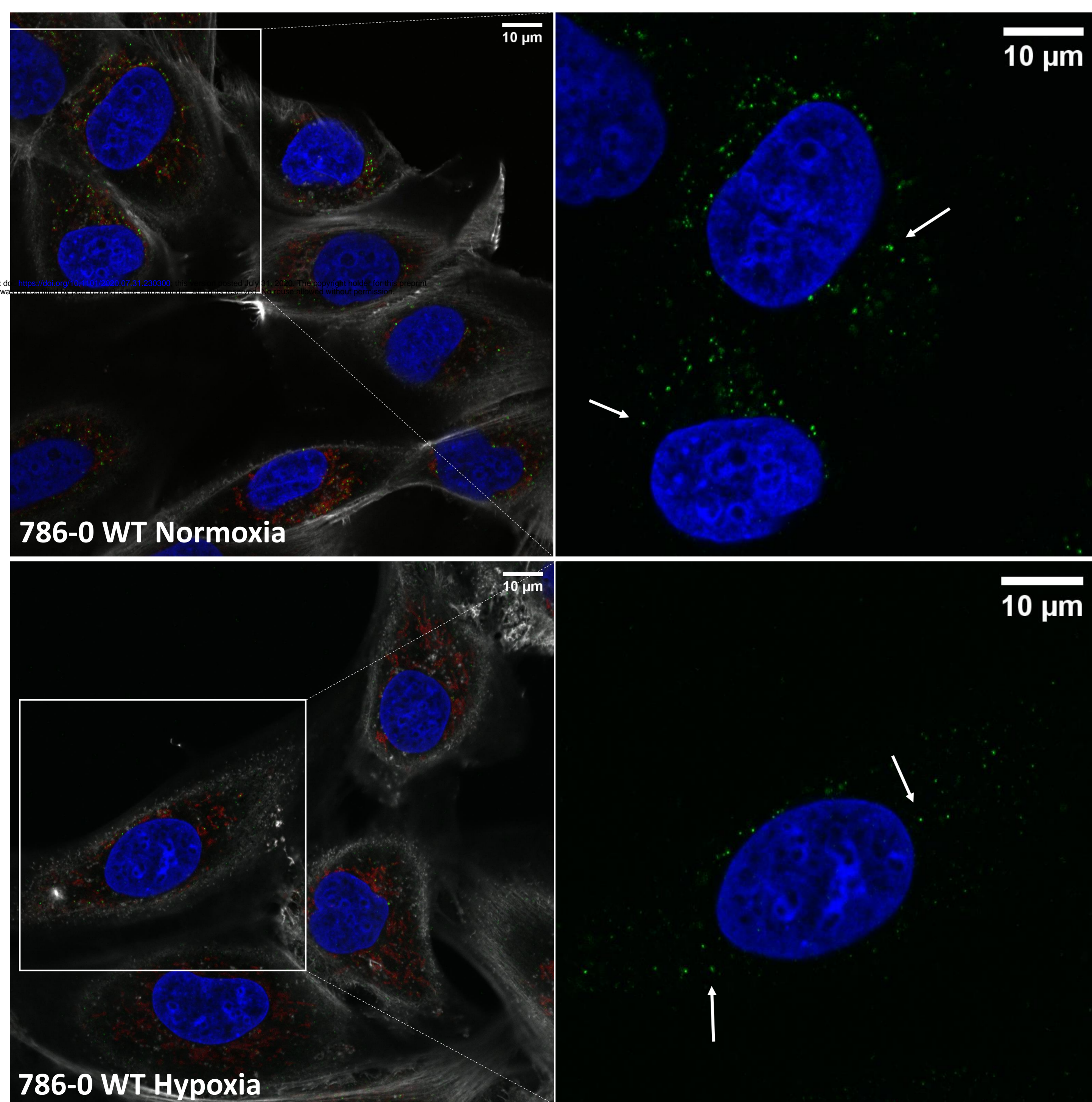
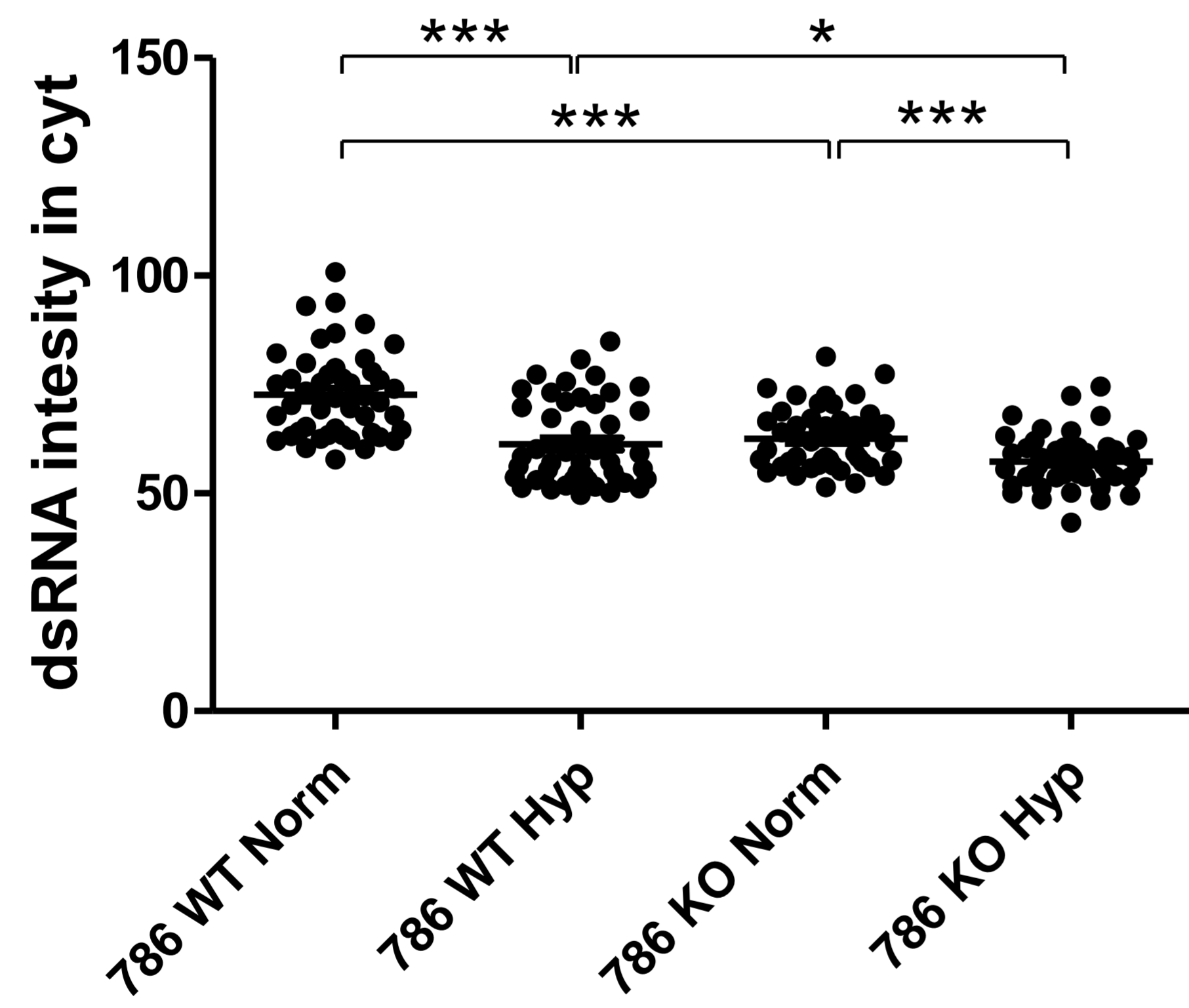


Figure 3

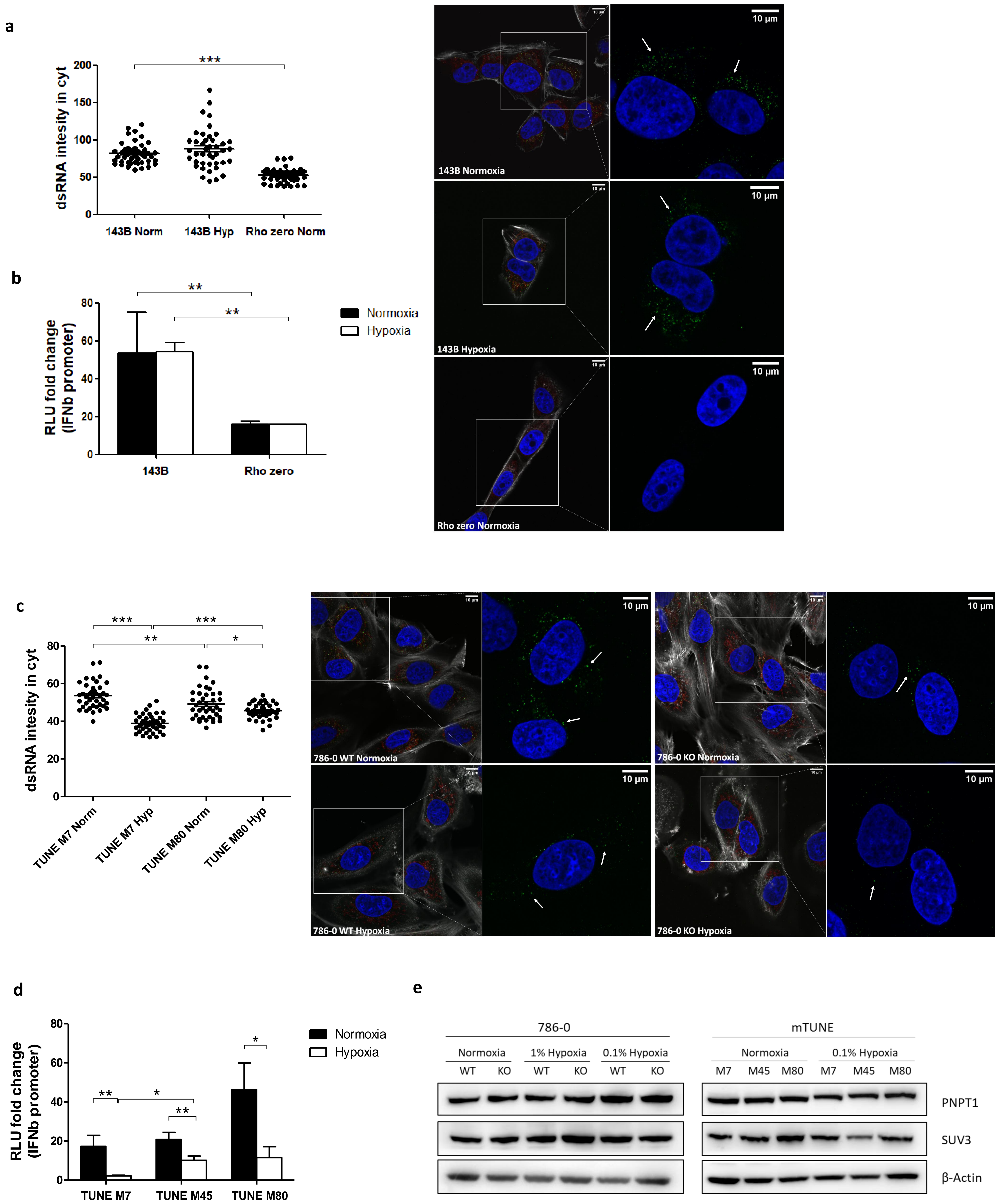
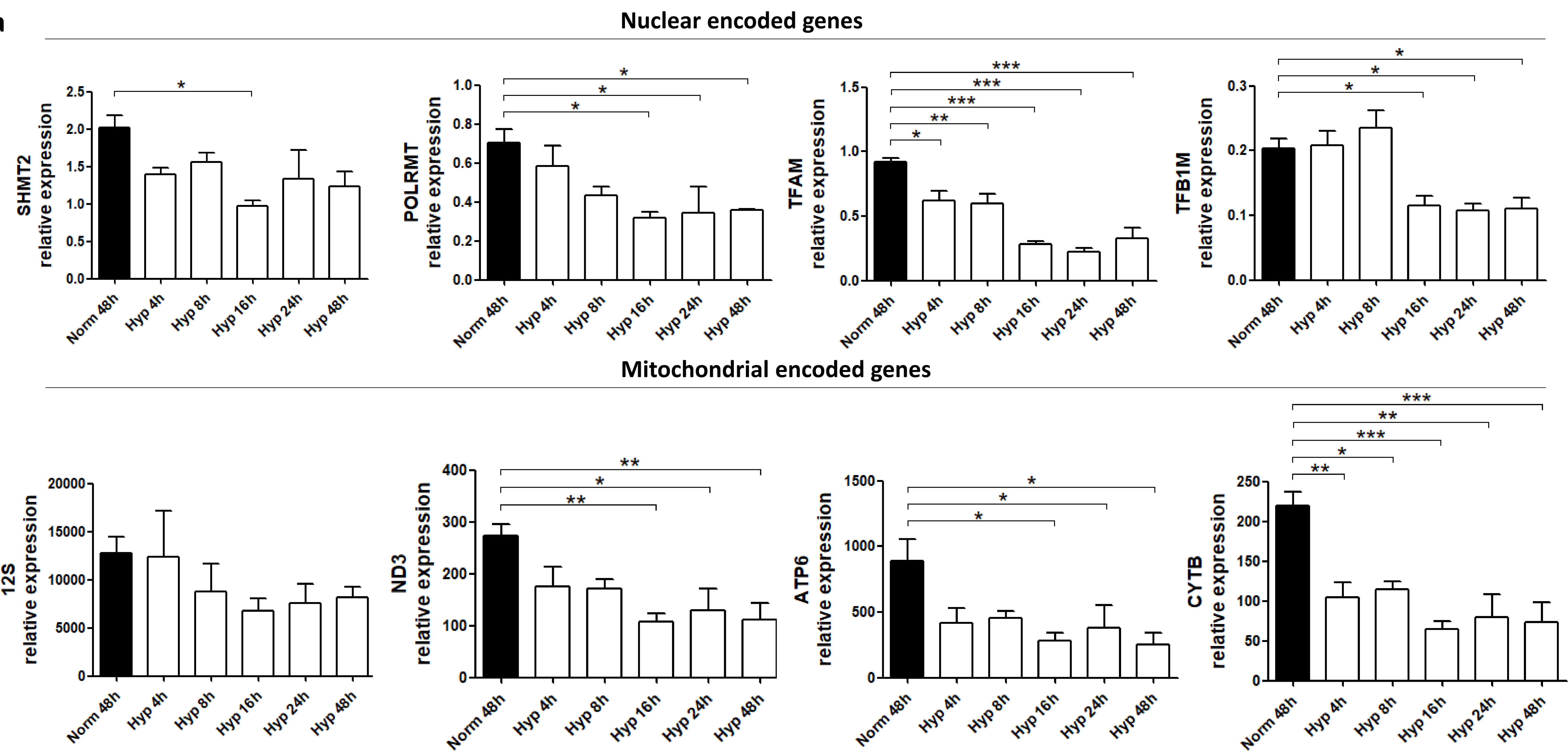


Figure 4

a



b

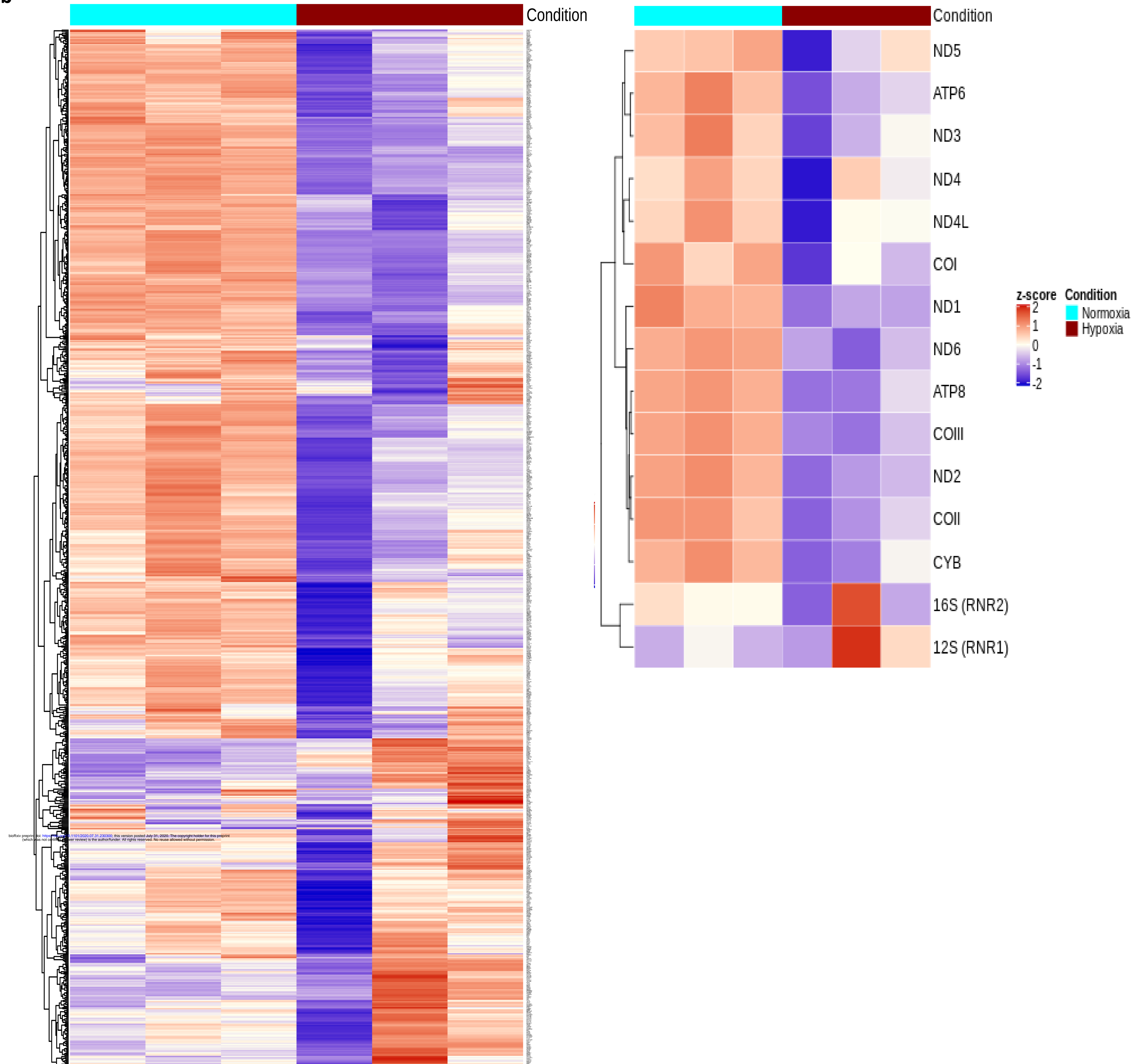
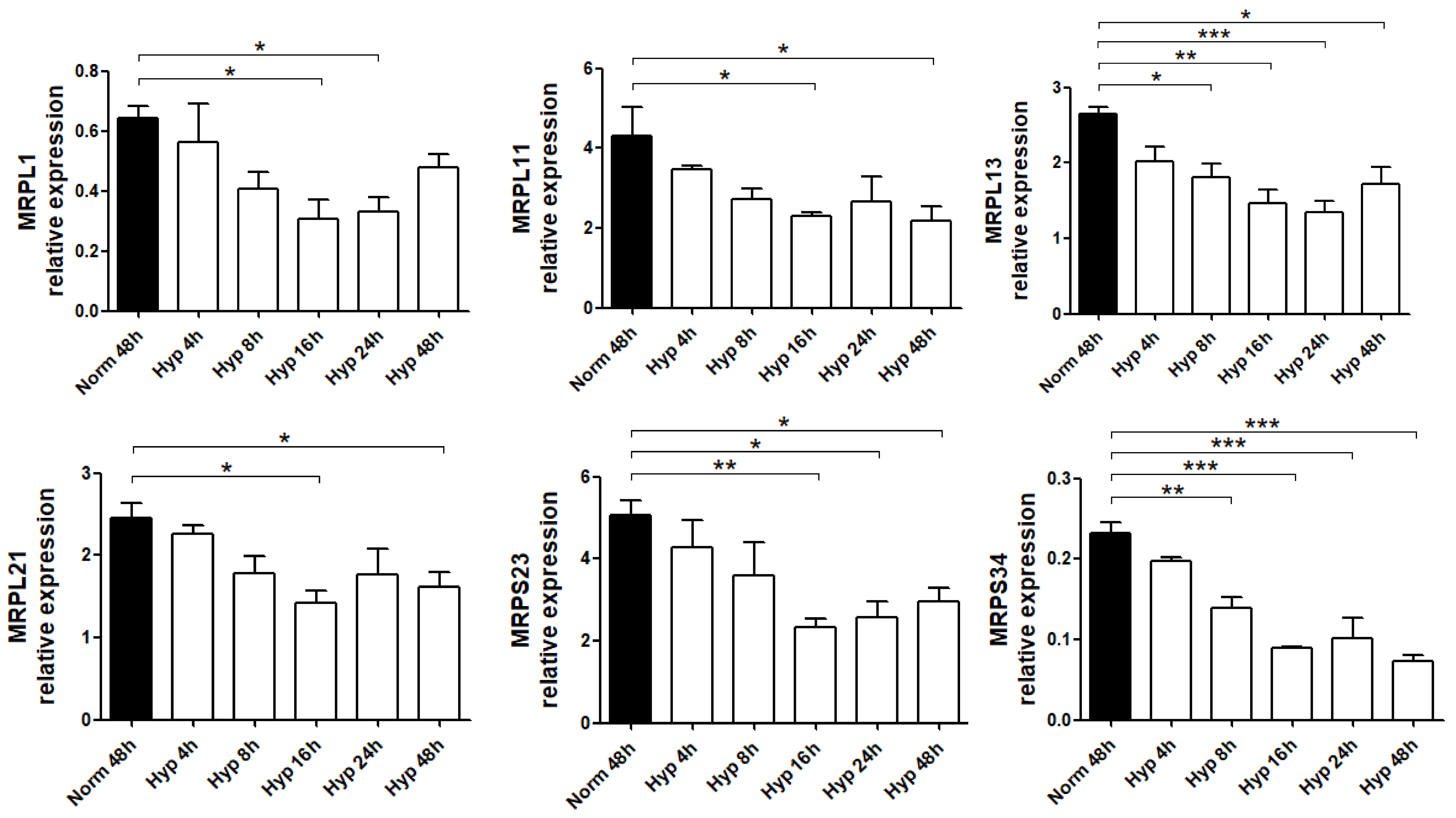


Figure 5

a



b

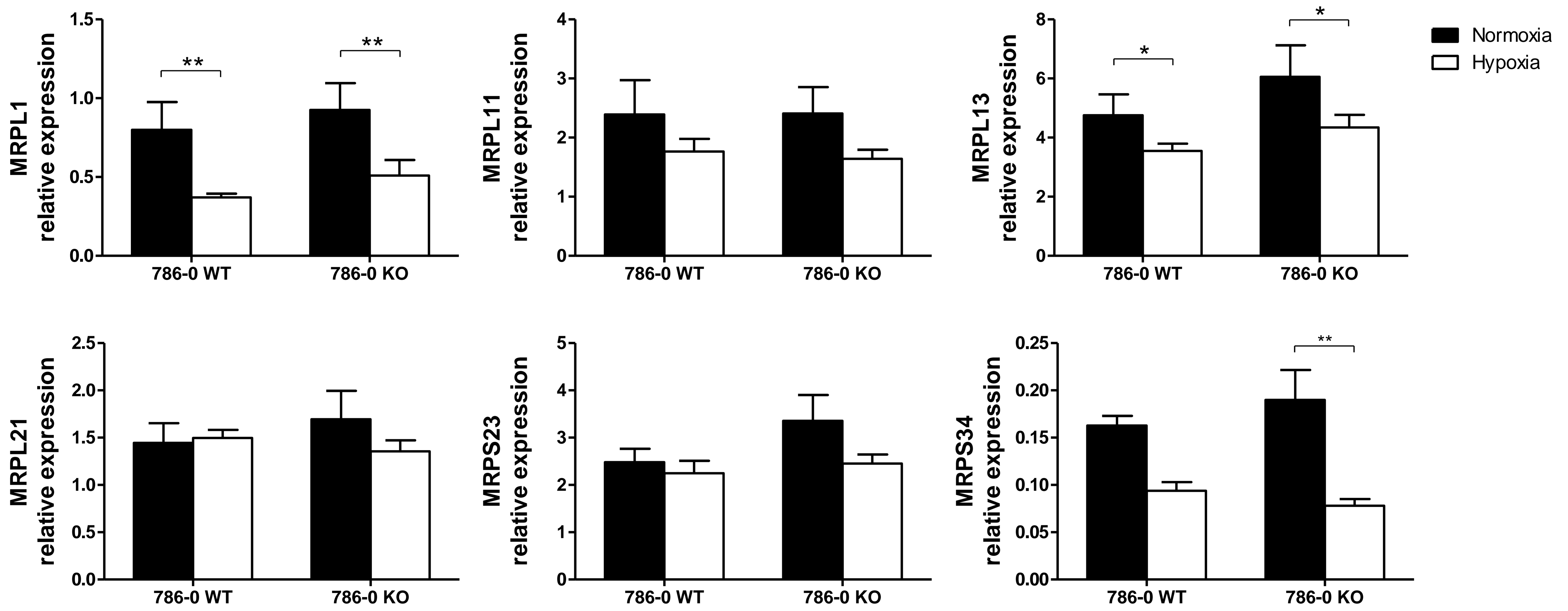


Figure 6

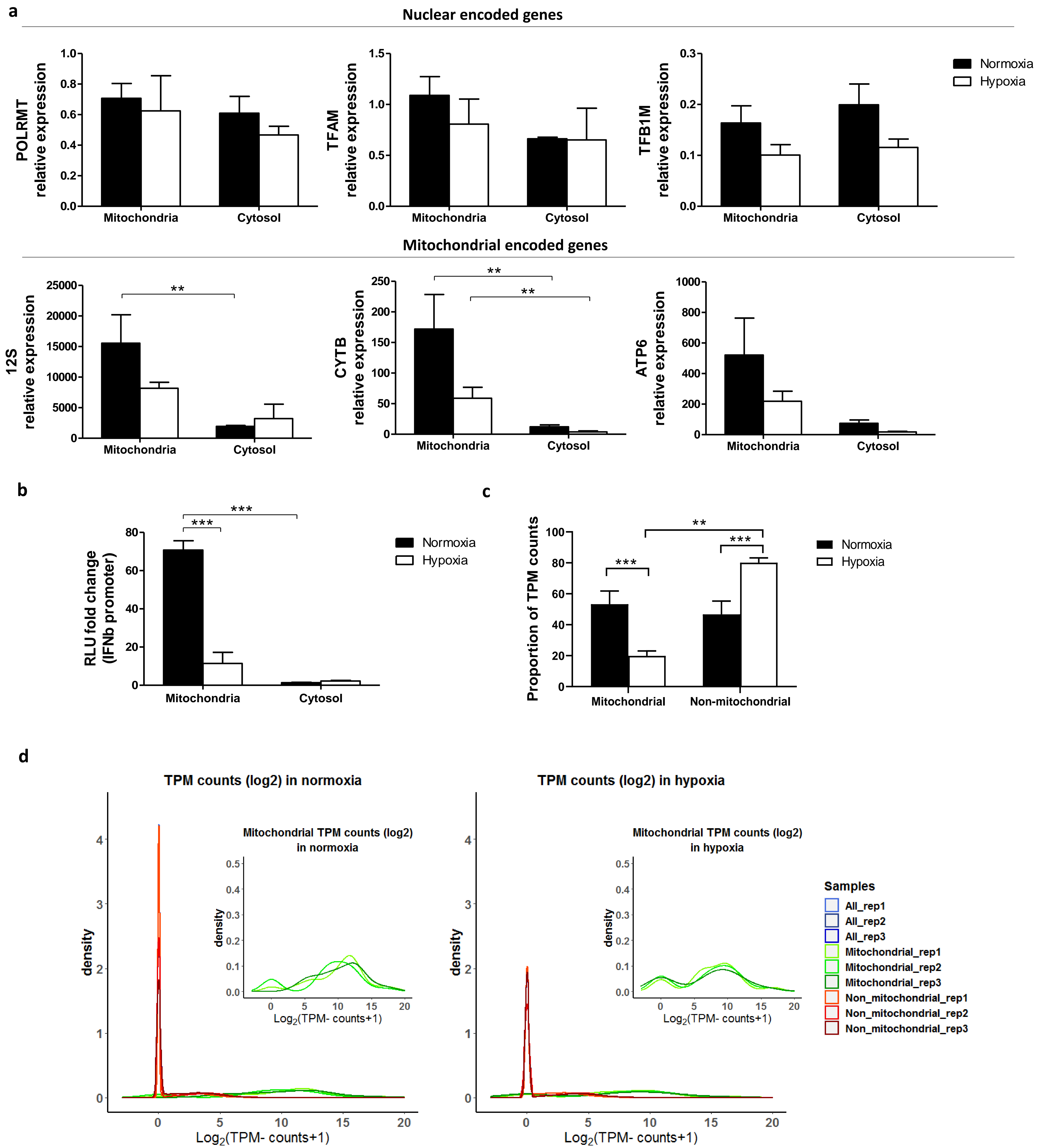
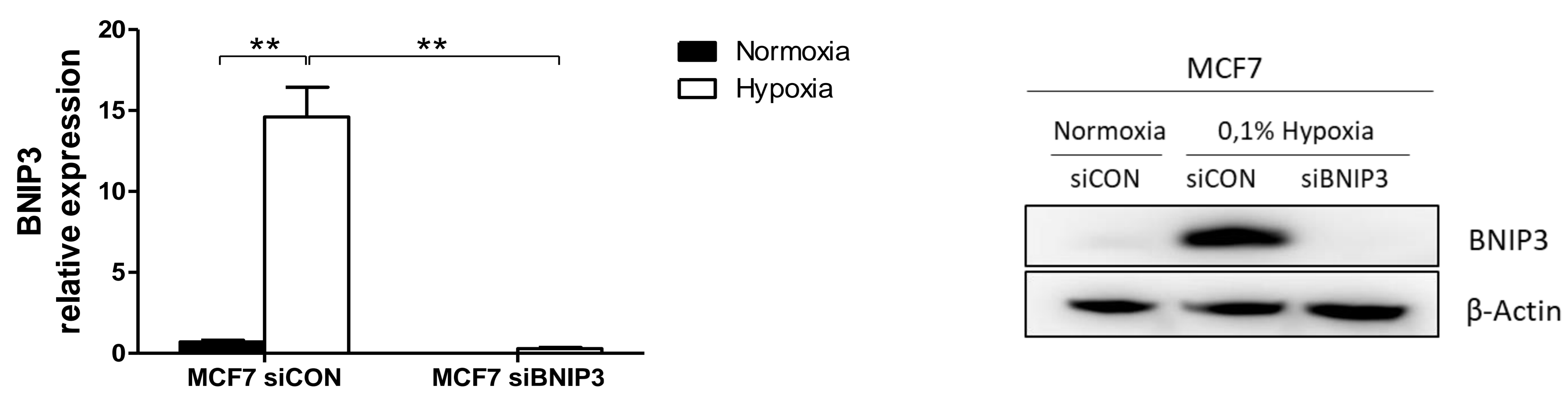
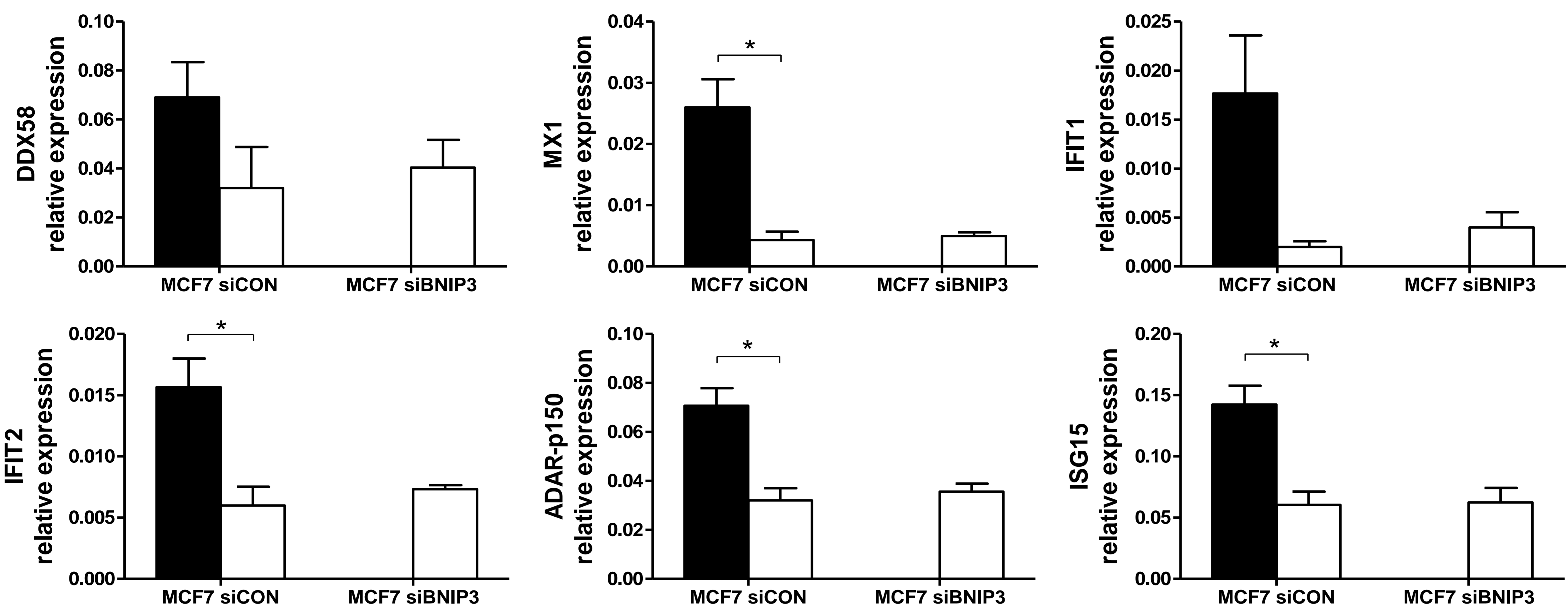


Figure 7

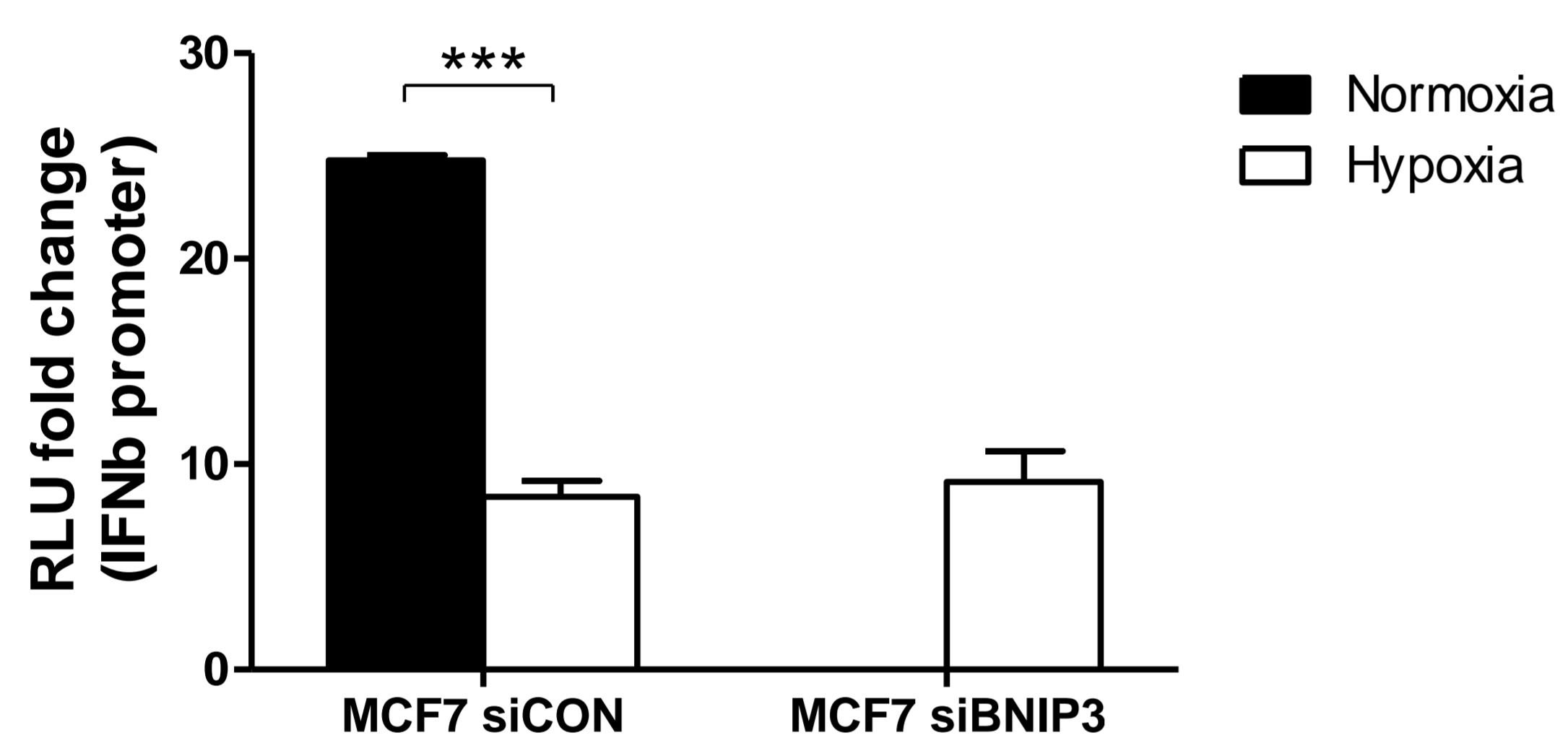
a



b



c



d

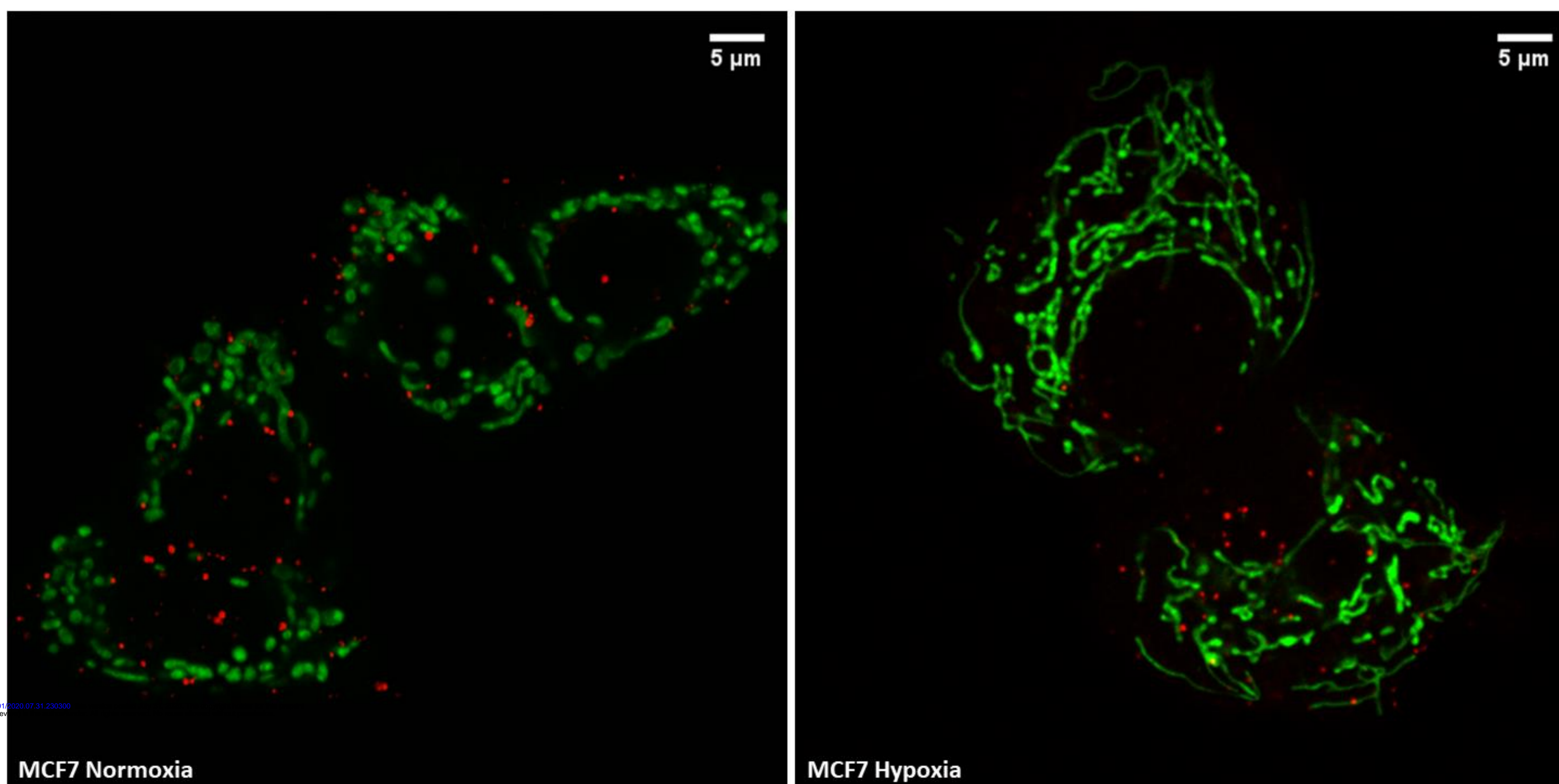


Figure 8

